

Comprehensive multiphase chlorine chemistry in the box model CAABA/MECCA: Implications to atmospheric oxidative capacity

Meghna Soni^{1, 2}, Rolf Sander³, Lokesh K Sahu¹, Domenico Taraborrelli⁴, Pengfei Liu⁵, Ankit Patel⁶, Imran A Girach⁷, Andrea Pozzer^{3, 8}, Sachin S Gunthe^{6, 9}, and Narendra Ojha¹

¹Physical Research Laboratory, Ahmedabad, India

²Indian Institute of Technology, Gandhinagar, India

³Atmospheric Chemistry Department, Max Planck Institute for Chemistry, Mainz, Germany

⁴Institute of Energy and Climate Research, Troposphere (IEK-8), Forschungszentrum Jülich GmbH, Jülich, Germany

⁵School of Earth and Atmospheric Sciences, Georgia Institute of Technology, Atlanta, GA, USA

⁶EWRE Division, Department of Civil Engineering, Indian Institute of Technology Madras, Chennai, India

⁷Space Applications Centre, Indian Space Research Organisation, Ahmedabad, India

⁸Climate and Atmosphere Research Center, The Cyprus Institute, Nicosia, Cyprus

⁹Centre for Atmospheric and Climate Sciences, Indian Institute of Technology Madras, Chennai, India

Correspondence: Meghna Soni (soni.meghna95@gmail.com) and Rolf Sander (rolf.sander@mpic.de)

Abstract. Tropospheric chlorine chemistry can strongly impact the atmospheric oxidation capacity and composition, especially in urban environments. To account for these reactions, the gas- and aqueous-phase Cl chemistry of the community atmospheric chemistry box model CAABA/MECCA has been extended. In particular, an explicit mechanism for ClNO₂ formation following N₂O₅ uptake to aerosols has been developed. The updated model has been applied to two urban environments with

5 different concentrations of NO_x (NO + NO₂): New Delhi (India) and Leicester (United Kingdom). The model shows a sharp build-up of Cl at sunrise through Cl₂ photolysis in both the urban environments. Besides Cl₂ photolysis, ClO+NO reaction,

and photolysis of ClNO₂ and ClONO are also prominent sources of Cl in Leicester. High-NO_x conditions in Delhi tend to suppress the night-time build-up of N₂O₅ due to titration of O₃ and thus lead to lower ClNO₂, in contrast to Leicester. Major loss of ClNO₂ is through its uptake on chloride, producing Cl₂, which consequently leads to the formation of Cl through photolysis.

10 The reactivities of Cl and OH are much higher in Delhi, however, the Cl/OH reactivity ratio is up to \approx 9 times greater in Leicester. The contribution of Cl to the atmospheric oxidation capacity is significant and even exceeds (by \approx 2.9 times) that of OH during the morning hours in Leicester. Sensitivity simulations suggest that the additional consumption of VOCs due to active gas- and aqueous-phase chlorine chemistry enhances OH, HO₂, and RO₂ near the sunrise. The simulation results of the updated model have important implications for future studies on atmospheric chemistry and urban air quality.

15 1 Introduction

Chlorine (Cl) radicals are one of the most important players in the tropospheric chemistry (Seinfeld and Pandis, 2016; Ravishankara, 2009). Cl impacts the oxidative capacity of the atmosphere, radical cycling, and, therefore, can significantly alter the atmospheric composition (Seinfeld and Pandis, 2016; Faxon and Allen, 2013). In comparison with hydroxyl (OH) radicals,

the so-called atmospheric detergent, the much faster reaction rates of Cl with volatile organic compounds (VOCs), enhance the 20 peroxy radicals (RO_2) formation and, thereby, the production of ozone (O_3) and secondary organic aerosols (SOA) (Qiu et al., 2019a; Choi et al., 2020). In addition, Cl radicals can also enhance the oxidation of climate-driving gases (such as methane and dimethyl sulphide) (Saiz-Lopez and von Glasow, 2012). Cl radicals are produced in the atmosphere through photochemistry involving heterogeneous reactions of Cl-containing gases and aerosols (Qiu et al., 2019a; Faxon and Allen, 2013). The major sources of Cl-containing species are anthropogenic activities in continental regions and sea salt aerosols in marine and 25 coastal environments (von Glasow and Crutzen, 2007; Osthoff et al., 2008; Liao et al., 2014; Liu et al., 2017; Thornton et al., 2010; Gunthe et al., 2021; Zhang et al., 2022). The photolysis of reactive Cl-containing species, such as chlorine gas (Cl_2), hypochlorous acid (HOCl), nitryl chloride (ClNO_2), and chlorine nitrite (ClONO) and the reaction of hydrochloric acid (HCl) with OH are known to produce Cl radicals in the lower troposphere (Atkinson et al., 2007; Riedel et al., 2014). With the rise in anthropogenic activities, emissions of Cl-containing species have increased significantly across the globe (Lobert et al., 1999; 30 Zhang et al., 2022), and hence the importance of Cl in local as well as regional atmospheric chemistry has become prominent.

Despite the aforementioned importance, Cl chemistry and associated ~~mechanism~~mechanisms, especially heterogeneous reactions in the lower troposphere, ~~however~~, are not yet fully understood, and the effects of Cl on atmospheric composition, air quality and oxidation capacity remain uncertain. Field measurements have revealed high concentrations of Cl species over 35 inland regions in addition to coastal and polar regions (von Glasow and Crutzen, 2007; Osthoff et al., 2008; Liao et al., 2014; Liu et al., 2017; Thornton et al., 2010), however, quantitative understanding of continental sources remains poorly understood. This is due to lack of the relevant heterogeneous and gas-phase chemistry in atmospheric photochemical models despite the range of chemical mechanisms complexity used in 3-D chemistry transport models (Xue et al., 2015; Pawar et al., 2023; Pozzer et al., 2022). In addition, the chemistry of Cl compounds has been less studied using the laboratory/chamber experiments. Qiu 40 et al. (2019b) showed that due to inadequate representation of heterogeneous Cl chemistry, the Community Multiscale Air Quality (CMAQ) model underestimated nitrate concentrations during daytime but overestimated during night-time in Beijing, China. In addition, the uncertainties associated with emission inventories of Cl species, can lead to inaccurate estimation of air composition (Zhang et al., 2022; Sharma et al., 2019). For example, Pawar et al. (2023) noticed that even after the inclusion of HCl emissions from trash burning the levels of nitrate, sulphate, nitrous acid (HONO) etc., still deviated from the observations 45 in Delhi, India, highlighting the need to include emissions from other sectors, such as industries. ~~Few~~A few recent studies assessed the impacts of the gas phase Cl chemistry by including gas phase ClNO_2 reactions, for example, Xue et al. (2015) reported about 25 % enhancement in the daytime oxidation of carbon monoxide and VOCs at a coastal site in East Asia. In the same region, the model predicted a 5-16 % enhancement in peak ozone with ClNO_2 ($\approx 50-200 \text{ pmol/mol}$) at a mountain top in Hong Kong, China (Wang et al., 2016). The measurements of Cl_2 (up to $\approx 450 \text{ pmol/mol}$) and ClNO_2 (up to $\approx 3.5 \text{ nmol/mol}$) 50 were reported from a rural site in the North China Plain and Cl chemistry was showed to enhance the formation of peroxy radicals (by 15 %) and O_3 production rate (by 19 %) (Liu et al., 2017).

Nevertheless, the heterogeneous chemistry of Cl species remains poorly represented in models, and often neglected in large scale numerical simulations. For example, in several models, the heterogeneous uptake of N_2O_5 on aqueous aerosols yielded 55 nitric acid (HNO_3) via reaction HET1:



However, N_2O_5 uptake on chloride-containing particles can produce ClNO_2 (Behnke et al., 1997; Thornton et al., 2010) especially in urban environments with strong NO_x emissions (Osthoff et al., 2008; Young et al., 2012). Incorporating heterogeneous mechanism of ClNO_2 into the regional models led to 3–12 % increase in O_3 over Northern China (Sarwar et al., 2014; 60 Zhang et al., 2017; Liu et al., 2017). In addition, heterogeneous reactions of Cl-containing species including particulate chloride (pCl^-), Cl_2 , ClNO_2 , chlorine nitrate (ClNO_3), and hypochlorous acid (HOCl) are suggested to result in the formation of Cl radicals as well as in recycling of NO_x , and HOx (OH , and HO_2) (Ravishankara, 2009; Qiu et al., 2019a; Hossaini et al., 2016; Faxon and Allen, 2013). Very recent measurements suggest a reduction in ClNO_2 formation due to the competition of N_2O_5 uptake among chloride, sulphate and acetate aerosols (Staudt et al., 2019). These heterogeneous reactions can be of paramount 65 significance in the Cl budget, however, to the best of our knowledge, these are not yet considered in model simulations.

The main goal of the present study is to investigate the role of chlorine chemistry in chemically contrasting urban environments. In this regard, we incorporate comprehensive gas-phase and heterogeneous Cl chemistry into a state of the art box model. Section 2 provides a detailed description of the Cl chemistry mechanism with gas-phase and heterogeneous reactions. 70 Section 3 describes the model setup and Section 4 shows the simulation results which include a detailed investigation on (i) the sensitivity of air composition to chlorine chemistry, (ii) the production and loss of Cl and ClNO_2 , (iii) the role of Cl in the Atmospheric Oxidative Capacity (AOC), and (iv) the sensitivity to $\text{ClNO}_2 + \text{Cl}^-$ reaction.

2 Mechanism Development

The community box model “Chemistry As A Boxmodel Application/Module Efficiently Calculating the Chemistry of the 75 Atmosphere” (CAABA/MECCA, Sander et al., 2019), has been used in this work. A comprehensive gas- and aqueous-phase mechanism of chlorine chemistry has been added to MECCA, here used within the box model CAABA. The gas-phase and heterogeneous chemistry implemented in MECCA is described in the following subsections and the full mechanism is shown in the supplementary section.

2.1 Gas-phase chlorine chemistry

80 A total of 36 inorganic, organic and photolysis reactions which are key contributors of Cl radicals were added to the mechanism (Table 1). The mechanism includes the inorganic reactions of Cl with NO_x , NO_3 (G1–G4), the reactions of Cl-containing species with OH and NO (G5–G7), and the reactions between Cl-containing species (G8–G9) (Qiu et al., 2019a; Burkholder et al., 2015; Atkinson et al., 2007). ClONO is formed through reaction of Cl with NO_2 (G2), and exists as a metastable

intermediate (Janowski et al., 1977; Niki et al., 1978; Golden, 2007). This intermediate subsequently transforms into ClNO_2 (G10), with an average conversion time of ≈ 12 h (ranging from 4 to 20 h), and the corresponding rate constant is 2.3 E-5 s^{-1} (Janowski et al., 1977). The Cl-initiated oxidation of organic species i.e. alkanes (C_3H_8 , C_4H_{10}), aromatics (benzene (C_6H_6), toluene (C_7H_8) and xylene (C_8H_{10})), alcohols (CH_3OH , $\text{C}_2\text{H}_5\text{OH}$), ketones (CH_3COCH_3 , MEK), isoprene (C_5H_8), and other organic compounds ($\text{C}_2\text{H}_5\text{CHO}$, HOCH_2CHO , BENZAL, GLYOX, MGLYOX) have also been included (G11–G31). The corresponding kinetic data are based on the International Union of Pure and Applied Chemistry and NASA Jet Propulsion Laboratory data evaluations (Atkinson et al., 2006, 2007; Burkholder et al., 2015), and from the literature (Niki et al., 1985, 1987; Green et al., 1990; Shi and Bernhard, 1997; Sokolov et al., 1999; Thiault et al., 2002; Wang et al., 2005; Rickard, 2009; Wennberg et al., 2018). In addition, photolysis reactions (G32–G36) resulting in production of Cl are also added to the module (Atkinson et al., 2007). The abbreviations of species mentioned in Table 1 are kept similar to that in the Master Chemical Mechanism (MCM) nomenclature (Rickard, 2009).

Table 1: Gas-phase chlorine reactions and corresponding rate constants added to MECCA. The rate constants are expressed in units of $\text{cm}^3 \text{ molecule}^{-1} \text{ s}^{-1}$ unless otherwise specified. Model-simulated maximum noontime J -values for Delhi are provided.

Reaction	Rate constant	Reference
Inorganic reactions		
(G1) $\text{Cl} + \text{NO} + \text{M} \rightarrow \text{ClNO}$	$7.6\text{E}(-32)*(\text{T}/300)^{-1.8}$	Qiu et al. (2019a)
(G2) $\text{Cl} + \text{NO}_2 + \text{M} \rightarrow \text{ClONO}$	1.6E-11	Burkholder et al. (2015)
(G3) $\text{Cl} + \text{NO}_2 + \text{M} \rightarrow \text{ClNO}_2$	3.6E-12	Burkholder et al. (2015)
(G4) $\text{Cl} + \text{NO}_3 \rightarrow \text{ClO} + \text{NO}_2$	2.40E-11 Qiu et al. (2019a)	
(G5) $\text{Cl}_2 + \text{OH} \rightarrow \text{HOCl} + \text{Cl}$	$3.6\text{E-12}*\text{exp}(-1200/\text{T})$	Atkinson et al. (2007)
(G6) $\text{ClNO}_2 + \text{OH} \rightarrow \text{HOCl} + \text{NO}_2$	$2.4\text{E-12}*\text{exp}(-1250/\text{T})$	Atkinson et al. (2007)
(G7) $\text{OCIO} + \text{NO} \rightarrow \text{NO}_2 + \text{ClO}$	$1.1\text{E-13}*\text{exp}(350/\text{T})$	Atkinson et al. (2007)
(G8) $\text{Cl} + \text{Cl}_2\text{O} \rightarrow \text{Cl}_2 + \text{ClO}$	$6.2\text{E-11}*\text{exp}(130/\text{T})$	Atkinson et al. (2007)
(G9) $\text{ClO} + \text{OCIO} + \text{M} \rightarrow \text{Cl}_2\text{O}_3$	1.2E-12	Atkinson et al. (2007)
(G10) $\text{ClONO} \rightarrow \text{ClNO}_2$	2.3E-5 s^{-1}	Janowski et al. (1977)
Organic reactions		
(G11) $\text{Cl} + \text{C}_3\text{H}_8 \rightarrow \text{iso-C}_3\text{H}_7\text{O}_2 + \text{HCl}$	$1.4\text{E-10} * 0.43 * \text{exp}(75/\text{T})$	Rickard (2009)
(G12) $\text{Cl} + \text{C}_3\text{H}_8 \rightarrow \text{n-C}_3\text{H}_7\text{O}_2 + \text{HCl}$	$1.4\text{E-10} * 0.59 * \text{exp}(-90/\text{T})$	Rickard (2009)
(G13) $\text{Cl} + \text{iso-C}_4\text{H}_{10} \rightarrow \text{iso-C}_4\text{H}_9\text{O}_2 + \text{HCl}$	$1.43\text{E-10} * 0.564$	Rickard (2009)
(G14) $\text{Cl} + \text{iso-C}_4\text{H}_{10} \rightarrow \text{tert-C}_4\text{H}_9\text{O}_2 + \text{HCl}$	$1.43\text{E-10} * 0.436$	Rickard (2009)
(G15) $\text{Cl} + \text{n-C}_4\text{H}_{10} \rightarrow \text{LC}_4\text{H}_9\text{O}_2 + \text{HCl}$	2.05E-10	Atkinson et al. (2006), Rickard (2009)
(G16) $\text{Cl} + \text{benzene} \rightarrow \text{C}_6\text{H}_5\text{O}_2 + \text{HCl}$	1.3E-16	Sokolov et al. (1999)

(G17)	$\text{Cl} + \text{toluene} \rightarrow \text{C}_6\text{H}_5\text{CH}_2\text{O}_2 + \text{HCl}$	6.20E-11	Wang et al. (2005)
(G18)	$\text{Cl} + \text{isoprene} \rightarrow .63 \text{ LISOPAB} + .30 \text{ LISOPCD} + .07 \text{ LISOPEFO2} + \text{HCl}$	$7.6\text{E-11} * \exp(500/T) * 1.1 * \exp(-595/T)$	Wennberg et al. (2018)
(G19)	$\text{Cl} + \text{isoprene} \rightarrow .63 \text{ LISOPAB} + .30 \text{ LISOPCD} + .07 \text{ LISOPEFO2} + \text{LCHLORINE}$	$7.6\text{E-11} * \exp(500/T) * (1 - 1.1 * \exp(-595/T))$	Wennberg et al. (2018)
(G20)	$\text{Cl} + \text{xylene} \rightarrow \text{C}_6\text{H}_5\text{CH}_2\text{O}_2 + \text{LCAR-BON} + \text{HCl}$	1.50E-10	Shi and Bernhard (1997)
(G21)	$\text{Cl} + \text{CH}_3\text{OH} \rightarrow \text{HOCH}_2\text{O}_2 + \text{HCl}$	$7.1\text{E-11} * 0.59 * \exp(-75/T)$	Atkinson et al. (2006)
(G22)	$\text{Cl} + \text{C}_2\text{H}_5\text{OH} \rightarrow \text{HOCH}_2\text{CH}_2\text{O}_2 + \text{HCl}$	$6.0\text{E-11} * \exp(155/T) * 0.28 * \exp(-350/T)$	Atkinson et al. (2006)
(G23)	$\text{Cl} + \text{C}_2\text{H}_5\text{OH} \rightarrow \text{C}_2\text{H}_5\text{O}_2 + \text{HCl}$	$6.0\text{E-11} * \exp(155/T) * (1 - 0.28 * \exp(-350/T))$	Atkinson et al. (2006)
(G24)	$\text{Cl} + \text{HOCH}_2\text{CHO} \rightarrow \text{HOCHCHO} + \text{HCl}$	$8.0\text{E-12} / 0.9 * 0.35$	Atkinson et al. (2006), Niki et al. (1987)
(G25)	$\text{Cl} + \text{HOCH}_2\text{CHO} \rightarrow \text{HOCH}_2\text{CO} + \text{HCl}$	$8.0\text{E-12} / 0.9 * (1 - 0.35)$	Atkinson et al. (2006), Niki et al. (1987)
(G26)	$\text{Cl} + \text{GLYOX} \rightarrow \text{HCOCO} + \text{HCl}$	3.8E-11	Niki et al. (1985)
(G27)	$\text{Cl} + \text{MGLYOX} \rightarrow \text{CH}_3\text{CO} + \text{CO} + \text{HCl}$	4.8E-11	Green et al. (1990)
(G28)	$\text{Cl} + \text{C}_2\text{H}_5\text{CHO} \rightarrow \text{C}_2\text{H}_5\text{CO}_3 + \text{HCl}$	1.3E-10	Atkinson et al. (2006)
(G29)	$\text{Cl} + \text{CH}_3\text{COCH}_3 \rightarrow \text{CH}_3\text{COCH}_2\text{O}_2 + \text{HCl}$	$1.5\text{E-11} * \exp(-590/T)$	Atkinson et al. (2006)
(G30)	$\text{Cl} + \text{MEK} \rightarrow \text{LMEKO}_2 + \text{HCl}$	$3.05\text{E-11} * \exp(80/T)$	Atkinson et al. (2006)
(G31)	$\text{Cl} + \text{BENZAL} \rightarrow \text{C}_6\text{H}_5\text{CO}_3 + \text{HCl}$	1.0E-10	Thiault et al. (2002)

Photolysis reactions		<i>J</i>-value (s⁻¹)	
(G32)	$\text{ClO} \rightarrow \text{Cl} + \text{O}_3\text{P}$	1.45E-4	Atkinson et al. (2007)
(G33)	$\text{Cl}_2\text{O} \rightarrow \text{Cl} + \text{ClO}$	9.20E-4	Atkinson et al. (2007)
(G34)	$\text{Cl}_2\text{O}_3 \rightarrow \text{ClO} + \text{ClO}_2$	5.50E-4	Atkinson et al. (2007)
(G35)	$\text{ClNO} \rightarrow \text{Cl} + \text{NO}$	2.89E-3	Atkinson et al. (2007)
(G36)	$\text{ClONO} \rightarrow \text{Cl} + \text{NO}_2$	3.81E-3	Atkinson et al. (2007)

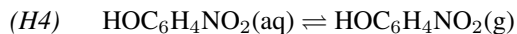
95 2.2 Heterogeneous chemistry

The aqueous-phase and heterogeneous chemistry of Cl compounds added to the MECCA is described in Table 2. In the present study, we assume that N_2O_5 is in equilibrium between the gas- and aqueous-phase (H2) according to Henry's law and the dissociation of $\text{N}_2\text{O}_5(\text{aq})$ to nitronium ion (NO_2^+) and nitrate (NO_3^-), occurs according to reaction (A1). The rate constant for the recombination reaction of NO_2^+ and NO_3^- is $2.7 \times 10^8 \text{ mol}^{-1} \text{ L s}^{-1}$, calculated based on Bertram and Thornton (2009);

100 Staudt et al. (2019). The acid dissociation of nitric acid (HNO_3) in aqueous phase (A3) also results in formation of NO_2^+ (Sapoli et al., 1985).

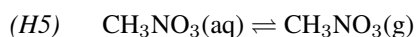
Table 2: Aqueous-phase and heterogeneous chlorine reactions added to MECCA

Reaction	Rate constant	Reference
Aqueous-phase reactions		
(A1) $\text{N}_2\text{O}_5(\text{aq}) \rightarrow \text{NO}_2^+(\text{aq}) + \text{NO}_3^-(\text{aq})$	$1.5 \times 10^5 \text{ s}^{-1}$	Staudt et al. (2019)
(A2) $\text{NO}_2^+(\text{aq}) + \text{NO}_3^-(\text{aq}) \rightarrow \text{N}_2\text{O}_5(\text{aq})$	$2.7 \times 10^8 \text{ mol}^{-1} \text{ L s}^{-1}$	Bertram and Thornton (2009); Staudt et al. (2019)
(A3) $\text{HNO}_3(\text{aq}) + \text{H}^+(\text{aq}) \rightarrow \text{NO}_2^+(\text{aq}) + \text{H}_2\text{O}(\text{aq})$	$1.6 \times 10^9 \text{ mol}^{-1} \text{ L s}^{-1}$	Sapoli et al. (1985)
(A4) $\text{NO}_2^+(\text{aq}) + \text{Cl}^-(\text{aq}) \rightarrow \text{ClNO}_2(\text{aq})$	$7.5 \times 10^9 \text{ mol}^{-1} \text{ L s}^{-1}$	Staudt et al. (2019)
(A5) $\text{ClNO}_2(\text{aq}) \rightarrow \text{NO}_2^+(\text{aq}) + \text{Cl}^-(\text{aq})$	$2.70 \times 10^2 \text{ s}^{-1}$	Behnke et al. (1997)
(A6) $\text{ClNO}_2(\text{aq}) + \text{Cl}^-(\text{aq}) \rightarrow \text{Cl}_2(\text{aq}) + \text{NO}_2^-(\text{aq})$	$10^7 \text{ mol}^{-1} \text{ L s}^{-1}$	Roberts et al. (2008)
(A7) $\text{OH}\cdot\text{Cl}^-(\text{aq}) + \text{OH}\cdot\text{Cl}^-(\text{aq}) \rightarrow \text{Cl}_2(\text{aq}) + 2 \text{OH}^-(\text{aq})$	$1.8 \times 10^9 \text{ mol}^{-1} \text{ L s}^{-1}$	Knipping et al. (2000)
(A8) $\text{OH}\cdot\text{Cl}^-(\text{aq}) + \text{Cl}^-(\text{aq}) \rightarrow \text{Cl}_2^-(\text{aq}) + 2 \text{OH}^-(\text{aq})$	$10^4 \text{ mol}^{-1} \text{ L s}^{-1}$	Grigorev et al. (1987)
(A9) $\text{Cl}_2^-(\text{aq}) + 2 \text{OH}^-(\text{aq}) \rightarrow \text{OH}\cdot\text{Cl}^-(\text{aq}) + \text{Cl}^-(\text{aq})$	$4.5 \times 10^7 \text{ mol}^{-1} \text{ L s}^{-1}$	Grigorev et al. (1987)
(A10) $\text{NO}_2^+(\text{aq}) + \text{H}_2\text{O}(\text{aq}) \rightarrow \text{HNO}_3(\text{aq}) + \text{H}^+(\text{aq})$	$1.6 \times 10^7 \text{ mol}^{-1} \text{ L s}^{-1}$	Staudt et al. (2019)
(A11) $\text{NO}_2^+(\text{aq}) + \text{SO}_4^{2-}(\text{aq}) \rightarrow \text{SO}_4^{2-}(\text{aq}) + \text{NO}_3^-(\text{aq}) + 2 \text{H}^+(\text{aq})$	$7.5 \times 10^9 \text{ mol}^{-1} \text{ L s}^{-1}$	Staudt et al. (2019)
(A12) $\text{NO}_2^+(\text{aq}) + \text{HCOO}^-(\text{aq}) \rightarrow \text{HCOO}^-(\text{aq}) + \text{NO}_3^-(\text{aq}) + 2 \text{H}^+(\text{aq})$	$7.5 \times 10^9 \text{ mol}^{-1} \text{ L s}^{-1}$	Staudt et al. (2019)
(A13) $\text{NO}_2^+(\text{aq}) + \text{CH}_3\text{COO}^-(\text{aq}) \rightarrow \text{CH}_3\text{COO}^-(\text{aq}) + \text{NO}_3^-(\text{aq}) + 2 \text{H}^+(\text{aq})$	$7.5 \times 10^9 \text{ mol}^{-1} \text{ L s}^{-1}$	Staudt et al. (2019)
(A14) $\text{NO}_2^+(\text{aq}) + \text{phenol}(\text{aq}) \rightarrow \text{HOC}_6\text{H}_4\text{NO}_2(\text{aq}) + \text{H}^+(\text{aq})$	$7.5 \times 10^9 \text{ mol}^{-1} \text{ L s}^{-1}$	Ryder et al. (2015); Heal et al. (2007)
(A15) $\text{NO}_2^+(\text{aq}) + \text{CH}_3\text{OH}(\text{aq}) \rightarrow \text{CH}_3\text{NO}_3(\text{aq}) + \text{H}^+(\text{aq})$	$4.5 \times 10^8 \text{ mol}^{-1} \text{ L s}^{-1}$	Iraci et al. (2007)
(A16) $\text{NO}_2^+(\text{aq}) + \text{CRESOL}(\text{aq}) \rightarrow \text{TOL1OHNO}_2(\text{aq}) + \text{H}^+(\text{aq})$	$7.5 \times 10^9 \text{ mol}^{-1} \text{ L s}^{-1}$	Coombes et al. (1979)
Heterogeneous reactions		
Henry's constant ($\text{mol L}^{-1} \text{ atm}^{-1}$)		
(H2) $\text{N}_2\text{O}_5(\text{g}) \rightleftharpoons \text{N}_2\text{O}_5(\text{aq})$	8.8E-2	Fried et al. (1994)
(H3) $\text{ClNO}_2(\text{g}) \rightleftharpoons \text{ClNO}_2(\text{aq})$	4.5E-2	Frenzel et al. (1998)



8.9E1

Müller and Heal (2001)



2.0E0

Sander (2015)

Thus produced nitronium ion (NO_2^+) reacts reversibly with chloride (Cl^-) yielding ClNO_2 (A4, A5) (Staudt et al., 2019; Behnke et al., 1997). After outgassing according to Henry's law (H3), ClNO_2 is photolyzed in the gas phase, producing Cl and NO_2 (Ghosh et al., 2012; Sander et al., 2014). ClNO_2 uptake on chloride containing aerosols results in formation of Cl_2 and nitrite ion (NO_2^-), as shown by the reaction (A6) (Roberts et al., 2008). Chamber experiments suggest the formation of Cl_2 from the self reaction of $\text{OH}\cdot\text{Cl}^-$ (A7), which gets formed via the reaction of OH with Cl^- (Knipping et al., 2000). Through other channel of reversible reactions (A8, A9), $\text{OH}\cdot\text{Cl}^-$ reacts with aqueous chloride and produces Cl_2^- , which can yield Cl_2 through subsequent reactions (Grigorev et al., 1987). The NO_2^+ uptake on aqueous chloride to form ClNO_2 (A4) is ≈ 500 times faster than NO_2^+ reaction with H_2O (A10) (Staudt et al., 2019). At the same time, experimental studies revealed a strong competition of NO_2^+ to react with Cl^- and with other nucleophiles (e.g. SO_4^{2-}) and aqueous organic compounds e.g. phenol, methanol, cresol (A11–A16) (Staudt et al., 2019; Ryder et al., 2015; Heal et al., 2007; Iraci et al., 2007; Coombes et al., 1979). These reactions could suppress the formation of ClNO_2 and also the corresponding rate constants for reactions A11–A14 are similar to the $\text{NO}_2^+ + \text{Cl}^-$ reaction yielding ClNO_2 i.e. $7.5 \times 10^9 \text{ mol}^{-1} \text{ L s}^{-1}$ (Staudt et al., 2019; Ryder et al., 2015; Heal et al., 2007). Methanol reacts with NO_2^+ (A15) and forms aqueous methyl nitrate (CH_3NO_3) (Iraci et al., 2007). Phase exchange for CH_3NO_3 and nitrophenol ($\text{HOC}_6\text{H}_4\text{NO}_2$) is shown by reactions H4 and H5, respectively. **Above discussed heterogeneous chemistry** The heterogeneous chemistry just discussed is implemented in MECCA and is summarized in Fig. 1. The rate constant for NO_2^+ reaction with methoxyphenol is about ≈ 10000 times smaller than NO_2^+ + phenol reaction (Kroflič et al., 2015), so it is not considered in this study. In addition, nitration reactions of other alcohols (e.g. catechol and polyphenols) could be potentially important, however due to unavailability of corresponding rate constants, these reactions are not considered in this study, nonetheless future studies calculating the kinetics of these reactions are recommended.

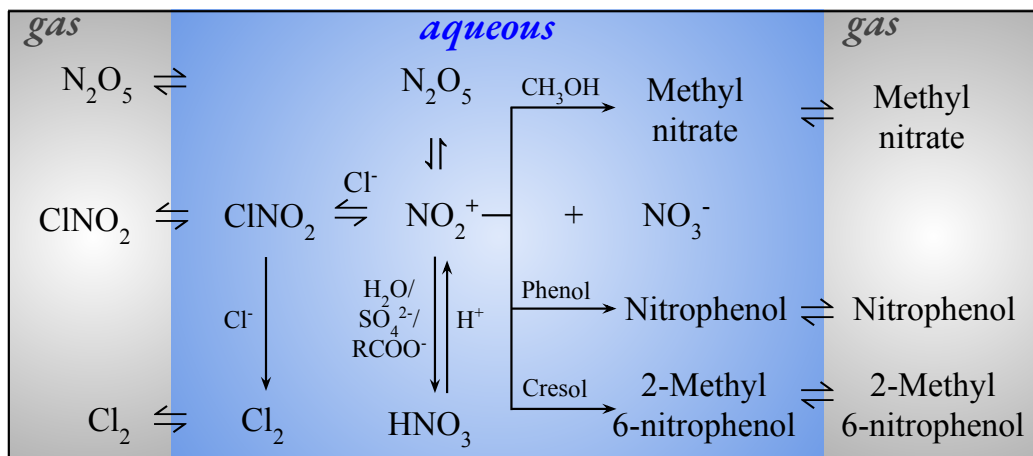


Figure 1. Aqueous-phase and heterogeneous chemistry added to MECCA.

120 In this study, Cl reacts with hydrocarbons and acetone via H-abstraction, and hence does not lead to the formation of any Cl-containing molecules, such as chloroacetone. This means that there are no such reactions in MECCA in which the Cl atom becomes part of the organic molecule. The reaction of Cl atoms with isoprene proceeds mainly via addition, and it produces chlorine-containing organics (Ragains and Finlayson-Pitts, 1997; Fan and Zhang, 2004). However, here we have simplified the mechanism by not considering the fate of organohalogens. Therefore, for future research, it would be valuable to investigate
125 the chemical kinetics of such reactions kinetics and their importance in the formation of organohalogen compounds.

3 Box model setup

The chemistry described in section 2 has been added into community box model CAABA/MECCA v4.4.2 (Sander et al., 2019). A comprehensive gas and aqueous phase tropospheric chemistry involving total 3330 reactions was utilized for the simulations, and the full set of reactions are presented in the electronic supplement. The gas-phase chemistry of organics like terpenes and
130 aromatics is treated by the Mainz Organic Mechanism (MOM) (Taraborrelli et al., 2012; Nölscher et al., 2014; Hens et al., 2014; Taraborrelli et al., 2021). The aqueous-phase chemistry of oxygenated VOCs is treated by the Jülich Atmospheric Mechanism of Organic Chemistry (JAMOC) (Rosanka et al., 2021). The numerical integration of the chemical mechanism is performed by the kinetic preprocessor v2.1 (KPP) (Sandu and Sander, 2006). The photolysis rate constants (J values) are calculated by the submodel JVAL, based on the method by Landgraf and Crutzen (1998). The Cl chemistry is expected to be more prominent
135 during winter conditions due to higher concentration of Cl-containing species in the boundary layer (Thornton et al., 2010; Gunthe et al., 2021; Sommariva et al., 2021), and therefore, simulations are performed for the winter season. Hence, the model is set-up for typical winter conditions of two different urban environments: Delhi (28.6° N, 77.2° E), India and Leicester (52.4° N, 01.1° W), United Kingdom. Simulations are performed for a 5-day period (17–21 February 2018) and output of 5th day has been considered for the analysis; by then, radicals had achieved almost a steady state. The typical environmental conditions
140 used in the simulations for Delhi (Tripathi et al., 2022) and Leicester (Sommariva et al., 2021) are summarized in Tab. 3 and Tab. S1.

VOC emissions are taken from the CAMS inventory (Sindelarova et al., 2014; Granier et al., 2019) and are adjusted iteratively in magnitude for better agreement with observations. CAMS-GLOB-ANT v5.3 (0.1° × 0.1°) (Granier et al., 2019) provides emissions of anthropogenic VOCs (e.g., benzene, toluene etc.), while emissions of biogenic VOCs (e.g., isoprene)
145 are from CAMS-GLOB-BIO v3.1 (0.25° × 0.25°) (Sindelarova et al., 2014). Emission of HCl and particulate chloride are included from Zhang et al. (2022) and adjusted iteratively towards reported levels of Cl-containing species (Gunthe et al., 2021; Sommariva et al., 2021). The Mainz Organic Mechanism (MOM) dry deposition scenario (Sander et al., 2019) is activated in the model. Ground-based lidar measurements of boundary layer height (BLH) during winter-time, performed as a part of the European Integrated project on Aerosol Cloud Climate and Air Quality Interactions (EUCAARI) project, are utilized for the
150 simulations at Delhi (Nakoudi et al., 2018). The diurnal variation in BLH in Leicester is extracted from the European centre for medium-range weather forecast's (ECMWF) fifth-generation reanalysis dataset ERA5 (Hersbach et al., 2020). Air compo-

Table 3. Environmental conditions of Delhi and Leicester in the model simulations.

Parameter	Delhi	Leicester
Latitude	28.58° N	52.38° N
Longitude	77.22° E	01.08° W
Time-zone	GMT+5:30	GMT+0:00
Temperature (K)	292	278.1
Pressure (mbar)	1010	1004
Air number density (molecules cm ⁻³)	2.5×10^{19}	2.61×10^{19}
Relative Humidity	67 %	90 %

sition in the model has been initialized based on previous studies (Tab. S1; Zhang et al. (2007); Lanz et al. (2010); Lawler et al. (2011); Sommariva et al. (2018, 2021); Gunthe et al. (2021); Tripathi et al. (2022)). The values of aerosol properties (e.g., radius, liquid water content, and chemical composition) incorporated in the simulations for both Delhi and Leicester as provided

155 in Table. S1. We constrained the model with the parameterized function best representing the observed diurnal variations of NO_x (Fig. 2) (Tripathi et al. (2022); Sommariva et al. (2018, 2021), <https://uk-air.defra.gov.uk/data/>) which helped in better reproducing the diurnal variations of some VOCs (e.g. isoprene) and ozone. Diurnal observations of HONO from Sommariva et al. (2021) are used for Leicester. For Delhi, however, HONO couldn't be constrained due to lack of observations.

4 Results and Discussion

160 The model captures the patterns in O₃ variability at both locations (Sommariva et al., 2018; Nelson et al., 2021; Chen et al., 2021; Sommariva et al., 2021; Nelson et al., 2023) to an extent, as shown in Fig. 2. O₃ is underestimated after \approx 16:00 h LT in Leicester mainly due to titration by high NO and lack of adequate dynamics/transport of O₃ in the model. Entrainment seems to improve O₃ after mid-night, towards the observed values (Fig. 2i). Simulated isoprene is in agreement with diurnal observations in Delhi (Tripathi et al., 2022) and in accordance with observed mean level in Leicester (Sommariva et al., 2021).
165 The nitrate radical (NO₃), which is a nighttime oxidant, is formed through reaction between NO₂ and O₃ (G37). NO₃ can react with NO₂ forming N₂O₅, which can again produce NO₃ and NO₂ through thermal dissociation (G38).



As seen in Fig. 2e, NO₃ remains negligible during the night-time (\approx 18:00–07:30 h LT) in Delhi due to unavailability of O₃ under high-NO conditions (up to 200 nmol/mol). Interestingly, despite its very short lifetime (\approx 5 s), about \approx 0.1 pmol/mol of NO₃ sustains during daytime. This is primarily due to prevailing levels of NO₂ (\approx 30 nmol/mol) and O₃ (\approx 40 nmol/mol).

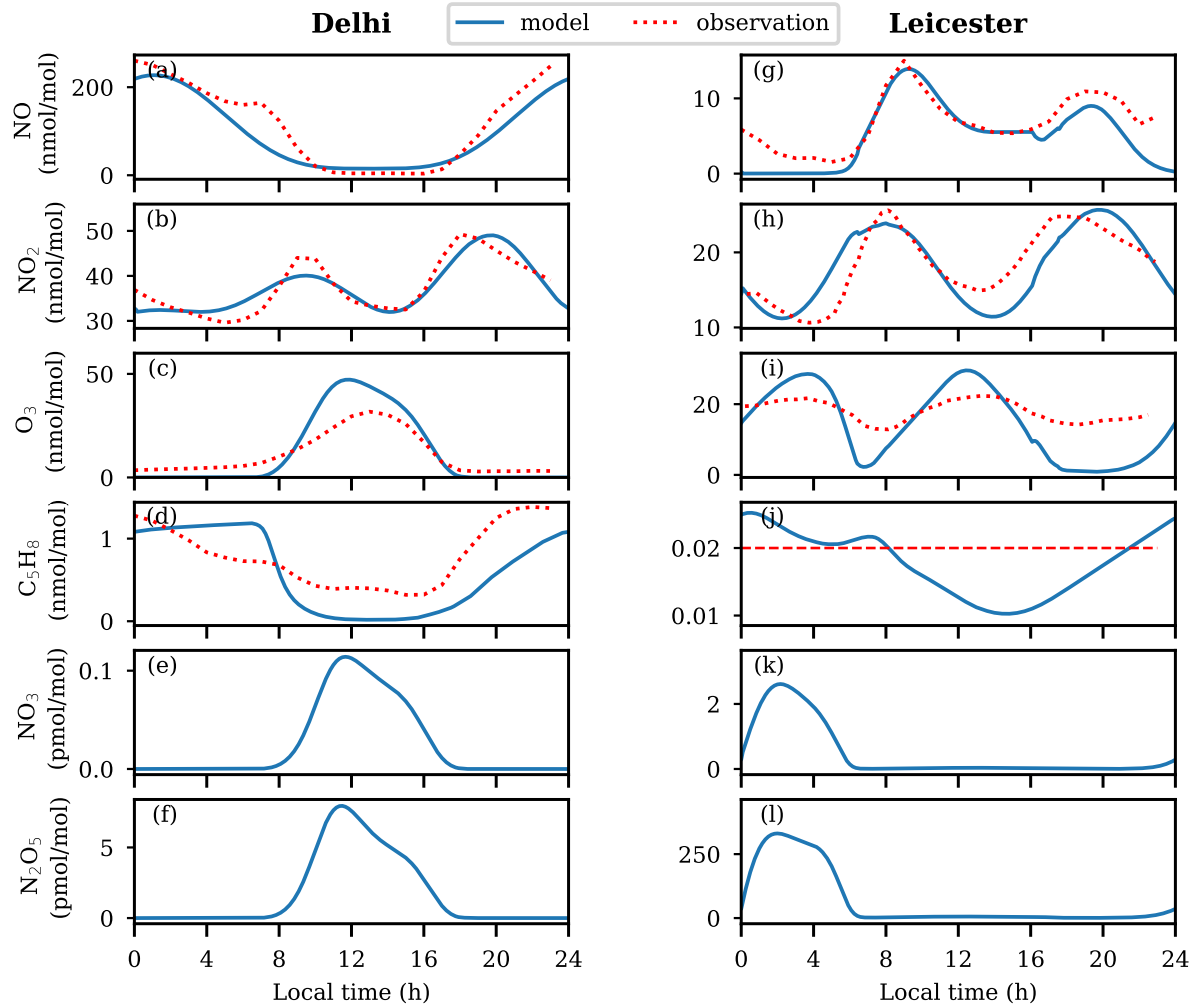


Figure 2. Diurnal variations of NO, NO₂, O₃, C₅H₈, NO₃, and N₂O₅ mixing ratios in Delhi (left) and Leicester (right). The unusual and negligible nighttime NO₃ in Delhi is attributed to the nearly non-existent O₃, due to titration by higher concentrations of NO. This leads to the negligible nighttime N₂O₅ in this region. Although mixing ratios of NO₃ and N₂O₅ peak during the daytime, their levels remain quite low. Mean value of observed C₅H₈ in Leicester is shown by red colored long dashed line.

Such unusual daytime enhanced NO₃ have been reported in recent studies, for example, 5-31 pmol/mol of NO₃ in Texas, USA (Geyer et al., 2003). Aircraft measurements during the New England Air Quality Study showed \approx 0.5 pmol/mol of NO₃ within boundary layer (\leq 1 km) during noon time (Brown et al., 2005). The calculated NO₃ levels using steady state approximation

175 showed 0.01-0.06 pmol/mol of NO₃ for the 1997-2012 period at urban sites in the UK (Marylebone Road London, London Eltham, and Harwell) (Khan et al., 2015a). Horowitz et al. (2007) suggested that NO₃ in tenths of pmol/mol during daytime over the eastern United States results in formation of \approx 50 % isoprene nitrates through oxidation of isoprene, which could

180 further affect the formation of O_3 and SOA significantly (Horowitz et al., 2007). Following to higher NO_3 , up to 8 pmol/mol of N_2O_5 is simulated during daytime in Delhi (Fig. 2f). Similar unusual daytime high levels of N_2O_5 ($\approx 21.9 \pm 29.3$ pptv) during wintertime were recently measured at Delhi using a high-resolution iodide adduct chemical ionization mass spectrometer (Haslett et al., 2023).

185 Enhanced NO_3 ≈ 2.6 pmol/mol and N_2O_5 ≈ 330 pmol/mol are simulated after mid-night in Leicester (Fig. 2k, 2l). In contrast to Delhi, the daytime simulated levels of NO_3 are negligible as it gets removed ~~fast rapidly~~ during the daytime by photolysis and through its reactions with NO , HO_2 , RO_2 , and VOCs (Khan et al., 2015b). In conjunction with high NO from $\approx 16:00$ h LT to near midnight that titrates O_3 , the corresponding NO_3 and N_2O_5 is negligible (following reactions G37 and G38). Night-time high and negligible day-time levels of NO_3 and N_2O_5 are their typical features which are generally reported in the literature (Brown et al., 2001; Seinfeld and Pandis, 2016).

190 4.1 Sensitivity of air composition to chlorine chemistry

195 To investigate the effects of Cl chemistry on air composition, other than comprehensive chemistry simulation discussed in previous section (simulation: NEW i.e. chemistry already present in the model + newly added gas and aqueous phase chlorine chemistry), two additional simulations have been performed, which are: (1) OLD – this includes default chemistry already present in the model, and (2) NOCL – OLD minus chlorine chemistry (i.e. without Cl chemistry). OLD simulation also encompassed some basic chlorine chemistry that was part of the model prior to its update (full mechanism is also shown in supplement). Figure 3 shows the comparison of Cl, $ClNO_2$, $ClONO$, OH, HO_2 , and RO_2 variations among the three simulations in Delhi and Leicester. Figure S5 shows the differences in diurnal variations of Cl, $ClONO + ClNO_2$, OH, HO_2 , and RO_2 in NEW simulation with: NOCL and OLD simulations.

200 The Delhi environment is mainly characterized by two peaks in Cl, a predominant sharp peak just after ~~the~~ sunrise followed by a broad shallow peak during noontime, corresponding to different mechanisms as discussed in the next section. With newly added chemistry (NEW simulation), a sharp peak in Cl is seen near ~~the~~ sunrise, with the maximum values attained is ≈ 3.5 fmol/mol (8.75×10^4 molec cm^{-3}) in Delhi (Fig. 3a). A broad smaller peak with magnitude of ≈ 0.8 fmol/mol maximizing around noontime is seen, which is ≈ 4 times smaller than the first morning peak. OLD simulation also show a sharp peak in 205 Cl near sunrise in Delhi, with a maximum of ≈ 11 fmol/mol (2.75×10^5 molec cm^{-3}). Cl get suppressed by up to ≈ 0.01 pmol/mol of maximum value in the OLD simulation, in the presence of added chlorine chemistry (NEW) as shown in Fig. S5. Similar to Cl, a peak is seen in $ClONO + ClNO_2$ of ≈ 100 pmol/mol with sunrise, which gradually decreases and attain ≈ 7 pmol/mol from nearly 11:00–16:00 h LT. Afterwards it increases to ≈ 20 pmol/mol from late evening as shown by Fig. 3b,c. The pathways for the formation of $ClNO_2$ and $ClONO$ were absent in earlier version of the model (OLD). Simulated OH, 210 HO_2 , and RO_2 show a prominent peak just after sunrise in the presence of Cl chemistry for both the OLD and NEW simulations (Fig. 3d,e,f). As a consequence of greater oxidation of VOCs by Cl, enhanced levels of OH by 0.05 pmol/mol (up to

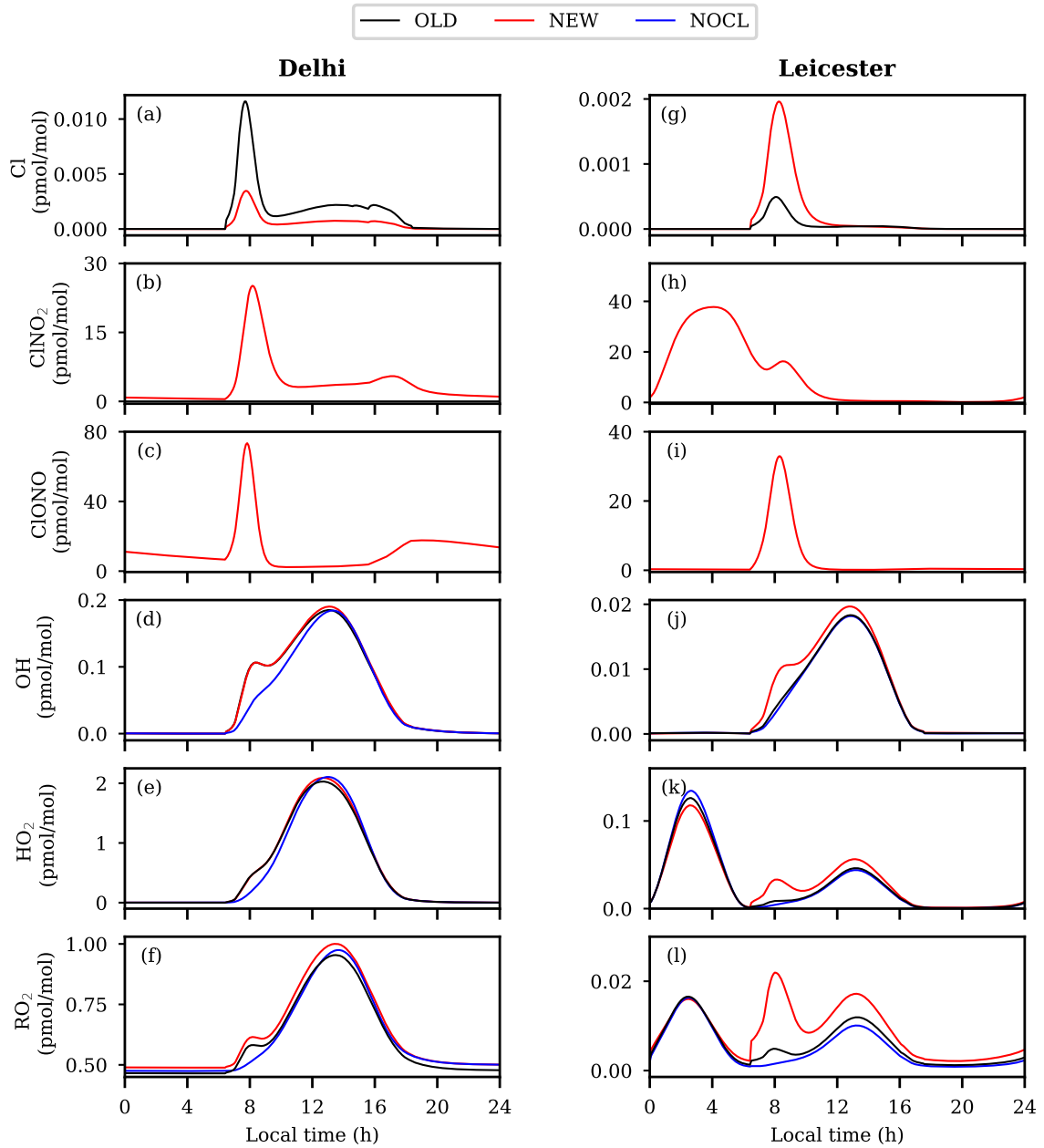


Figure 3. Model simulated diurnal variations of Cl, ClNO₂, ClONO, OH, HO₂, and RO₂ at Delhi (left panel) and Leicester (right panel).

a factor of ≈ 1.8), HO₂ by 0.21 pmol/mol and RO₂ by 0.1 pmol/mol are noted with added Cl chemistry compared to NOCL case (see Fig. S5). No significant changes are seen in noon-time levels of OH and HO₂, whereas ≈ 1.1 times more RO₂ is

produced with added Cl chemistry (NEW) compared to the OLD simulation.

215

The model-predicted Cl peaks at ≈ 2 fmol/mol (5.2×10^4 molec cm^{-3}) during sunrise in Leicester (Fig. 3g). In contrast to Delhi, suppressed Cl (up to ≈ 3.2 times) with a narrow peak is simulated by OLD simulation in comparison with NEW simulation containing newly added Cl chemistry, at Leicester. In contrast to negligible night-time $\text{ClONO} + \text{ClNO}_2$ in Delhi, it shows a strong build-up over Leicester during 0-4 hours with a maximum of ≈ 40 pmol/mol, with higher levels (up to 220 50 pmol/mol) prevailing until about sunrise. $\text{ClONO} + \text{ClNO}_2$ is negligible during mid-day until mid-night, in accordance with N_2O_5 in Leicester as shown in Fig. 2l. Previous studies have demonstrated that the formation of ClNO_2 occurs within the nocturnal residual layer, which contains lower levels of NO compared to the surface layer. Subsequently, ClNO_2 mixes downward during the morning when the convective mixed layer develops (Bannan et al., 2015; Tham et al., 2016). However, the present study does not account the the effect of transport processes due to the limitations of the box model. The effects 225 of added Cl chemistry on OH, HO_2 , and RO_2 are more prominent in Leicester compared to Delhi. NEW simulation show strong enhancements in OH (up to ≈ 2 times), HO_2 (up to ≈ 5 times), and RO_2 (up to ≈ 8 times) after sunrise which is gradually progressive, resulting in higher levels during noon-time as well (Fig. 3, Fig. S5). Remarkably elevated levels of 230 RO_2 (by a factor of ≈ 2) are prominent during the noon hours. Such elevated levels of RO_2 could favour enhanced levels of secondary organic aerosols in Leicester. The impact of Cl chemistry on aerosols (NO_2^+ , NO_3^- , and oxalic acid) is discussed in Supplementary section 2.2 (Fig. S6). Though significant differences in NO_2^+ , NO_3^- , and oxalic acid are seen due to Cl chemistry but, further measurements are required for validation. In the next sections, we have analysed the observed behaviour of Cl and ClNO_2 in the NEW simulation over both the locations in more detail.

4.2 Production and loss of Cl and ClNO_2

The sources and sinks of Cl in Leicester and Delhi are presented in Fig. 4. The left-upper ~~panels~~panel (a) delineates the sources 235 and sinks of Cl radical on diurnal scale in Delhi. The morning sharp peak in Cl radical is caused mainly by the photolysis of Cl_2 with a maximum rate of 1.2×10^7 molec $\text{cm}^{-3} \text{ s}^{-1}$. The shallow secondary peak is due to the reaction $\text{HCl} + \text{OH}$ with a noon time rate of $\approx 0.4 \times 10^7$ molec $\text{cm}^{-3} \text{ s}^{-1}$. However, there is a smaller contribution from other reactions (photolysis of ClNO_2 , ClONO and reaction of ClO with NO) to the morning peak, ~~while~~which have negligible contributions during the daytime. Interestingly, there is a strong consumption of Cl to oxidize VOCs (peak rate $\approx 2.4 \times 10^7$ molec $\text{cm}^{-3} \text{ s}^{-1}$) during 240 sunrise, and a lesser consumption during the rest of the day. $\text{Cl} + \text{NO}_2$ is also a Cl sink during the morning time in Delhi. The Cl-initiated oxidation of VOCs in the morning hours in Delhi may lead to formation of secondary organic aerosols and new particle formation, which opens up pathways of future research in this direction. In addition to Cl_2 photolysis ($\approx 1.0 \times 10^6$ molec $\text{cm}^{-3} \text{ s}^{-1}$), photolysis of ClNO_2 and ClONO , and $\text{ClO} + \text{NO}$ reaction (total rate $\approx 0.8 \times 10^6$ molec $\text{cm}^{-3} \text{ s}^{-1}$) are other prominent sources of Cl in Leicester. VOCs are the major sink for Cl (rate $\approx 1.3 \times 10^6$ molec $\text{cm}^{-3} \text{ s}^{-1}$), followed by 245 NO_2 (rate $\approx 0.6 \times 10^6$ molec $\text{cm}^{-3} \text{ s}^{-1}$).

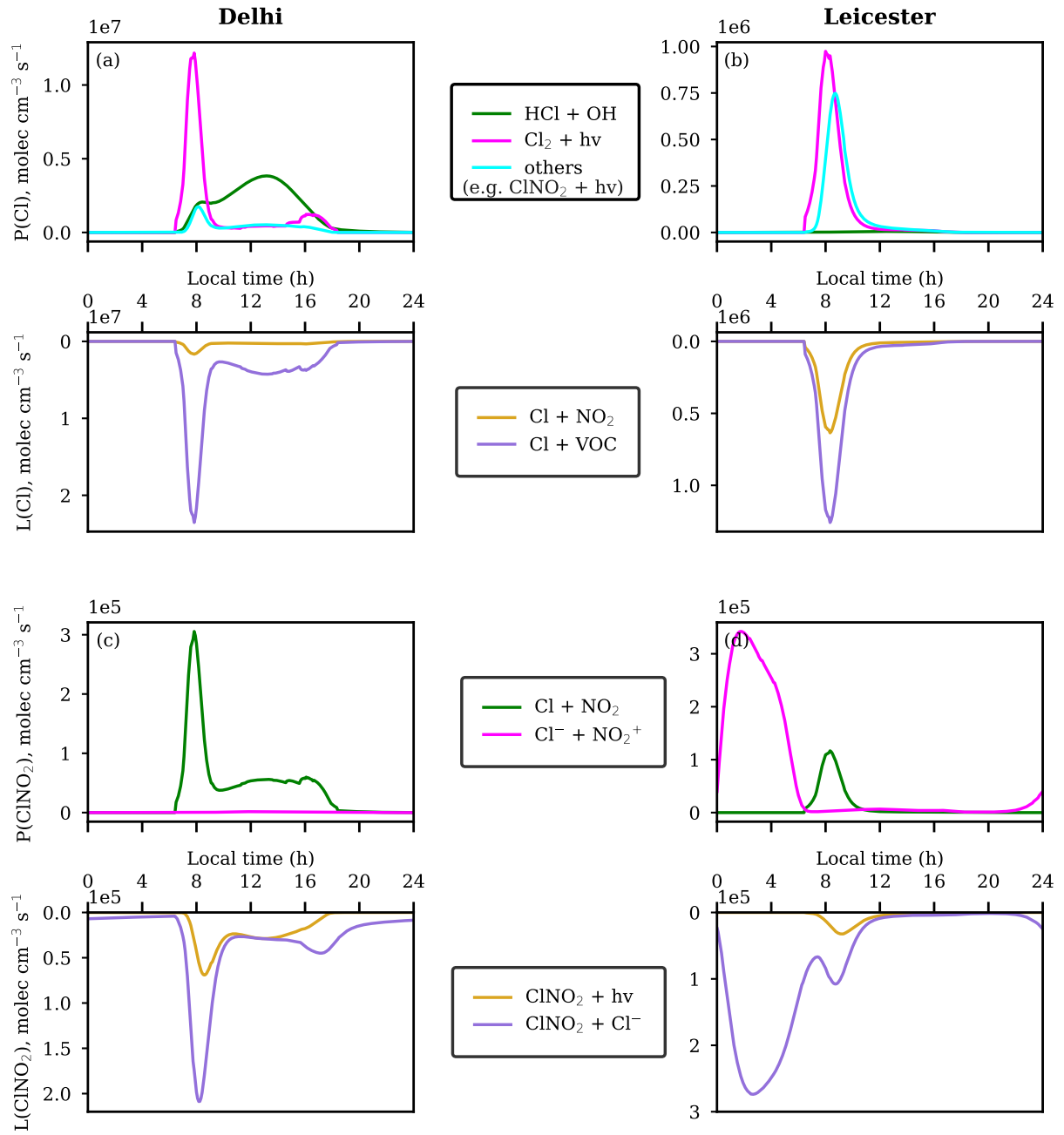


Figure 4. Production and loss rates of (a, b) Cl and (c, d) ClNO₂ in Delhi (left panel) and Leicester (right panel).

We further analyzed the production and loss pathways of ClNO₂, as shown in Fig. 4c,d. While the major source of ClNO₂ is through the Cl + NO₂ reaction with a reaction rate $\approx 3 \times 10^5$ molec $\text{cm}^{-3} \text{s}^{-1}$ in Delhi, the aqueous phase reaction Cl⁻ + NO₂⁺

($\approx 3.4 \times 10^5$ molec $\text{cm}^{-3} \text{ s}^{-1}$) is the prominent source in Leicester corresponding to the peak ClNO_2 (Fig. 2h,p). Though gas-phase reaction $\text{Cl} + \text{NO}_2$ is discussed in the literature (Burkholder et al., 2015; Qiu et al., 2019a), however, to the best of our knowledge, such an unusually higher contribution of this reaction (seen in Delhi) as compared to the aqueous-phase reaction of $\text{Cl}^- + \text{NO}_2^+$ has not been reported in any study. The reaction of Cl with NO_2 ($\approx 1.1 \times 10^5$ molec $\text{cm}^{-3} \text{ s}^{-1}$) is the major ClNO_2 source during the sunrise in Leicester. In contrast, there is lesser contribution of $\text{Cl}^- + \text{NO}_2^+$ reaction (rate $\approx 1 \times 10^3$ molec $\text{cm}^{-3} \text{ s}^{-1}$) in ClNO_2 production in Delhi. The prominent sink for ClNO_2 is through it's heterogeneous reaction with Cl^- ($\approx 1.8 \times 10^5$ molec $\text{cm}^{-3} \text{ s}^{-1}$ or 7.2×10^{-15} mol $\text{mol}^{-1} \text{ s}^{-1}$) in Delhi almost throughout the day, while it's loss through the photolysis ($\approx 0.5 \times 10^5$ molec $\text{cm}^{-3} \text{ s}^{-1}$ or 2×10^{-15} mol $\text{mol}^{-1} \text{ s}^{-1}$) is also an important sink during the daytime. We are using ClNO_2 uptake coefficient, $\gamma = 9\text{E-}3$ from Fickert et al. (1998) in the simulation. Sensitivity simulation with $\gamma = 1\text{E-}5$ (Haskins et al., 2019) results in considerably slower (by a factor of ≈ 270 and ≈ 17 , near sunrise and during mid-day, respectively) loss rate of ClNO_2 with Cl^- than in the NEW simulation over Delhi. ClNO_2 loss through the reaction $\text{ClNO}_2 + \text{Cl}^-$ ($\approx 2.7 \times 10^5$ molec $\text{cm}^{-3} \text{ s}^{-1}$ or 1.0×10^{-14} mol $\text{mol}^{-1} \text{ s}^{-1}$) is its major sink in Leicester from mid-night to mid-day, while photolysis ($\approx 0.3 \times 10^5$ molec $\text{cm}^{-3} \text{ s}^{-1}$ or 1.1×10^{-15} mol $\text{mol}^{-1} \text{ s}^{-1}$) is smaller sink from sunrise to mid-day here. The diurnal variation in Cl_2 , and its production and loss mechanisms over Delhi and Leicester are shown by Fig. S1 and Fig. S2. In conjunction with major loss of ClNO_2 , $\text{ClNO}_2 + \text{Cl}^-$ reaction is the major contributor to Cl_2 formation over Delhi and Leicester.

265

We also calculated ClNO_2 yield from NO_2^+ (Fig. S3), which is the ratio of $P_{\text{ClNO}_2}/L_{total}$, where P_{ClNO_2} is the rate of ClNO_2 production through $\text{Cl}^- + \text{NO}_2^+$ reaction and L_{total} denotes the loss rate of NO_2^+ through it's reactions with Cl^- , H_2O , SO_4^{2-} , HCOO^- , CH_3COO^- , phenol, CH_3OH , and cresol (A4, A10–A16). ClNO_2 yield is ≈ 0.9 over Delhi, indicating the strongest loss of NO_2^+ is through it's reaction with Cl^- , which is also mimicked in Fig. S4a showing the same concentrations of ClNO_2 as in NEW simulation and when other NO_2^+ reactions (A10–A16) are turned off (simulation: without other NO_2^+ reactions). ClNO_2 yield over Leicester is between ≈ 0.40 – 0.55 , which is about half the yield in Delhi. Stronger ClNO_2 yield in Delhi could be attributed to ≈ 2 times higher Cl^- than Leicester. Lesser ClNO_2 yield in Leicester portrays the importance of NO_2^+ loss reactions (A10–A15) other than with Cl^- , which could be seen through Fig. S4b where ClNO_2 is increased by more than twice during early morning hours when A10–A15 reactions are kept inactive in the model. The determination of ClNO_2 yield using cavity ring-down spectroscopy and chemical ionization mass spectrometry, shows yield ranging between 0.2 to 0.8 for Cl^- concentrations of 0.02 to 0.5 mol/L (Roberts et al., 2009). The measurements of ClNO_2 yield for coastal and open ocean waters were found to be between 0.16–0.30 which is suppressed by up to 5 times than equivalent salt containing solutions, due to the addition of aromatic organic compounds (e.g., phenol and humic acid) to synthetic seawater matrices (Ryder et al., 2015).

280 4.3 Role of Cl in Atmospheric Oxidative Capacity (AOC)

In order to understand the role of Cl as oxidising agent with respect to the OH radical, we calculated the reactivity of Cl and OH as $\sum_{X_i} (k_{\text{radical}+X_i} \times [X_i])$, where radical is Cl or OH, and $[X_i]$ is the concentration of specie X_i (here X_i includes CO,

CH₄, primary VOCs and NMHCs which are initialized in the model) (Fig. 5). The corresponding rate constants for Cl + X and OH + X reactions are taken from the MECCA. The reactivity of both Cl and OH decreases rapidly nearly from sunrise 285 to noon time and afterwards increases gradually at both locations. In comparison to Leicester, the magnitudes of Cl and OH reactivity in Delhi are higher by up to ≈ 1.4 and ≈ 12 times, respectively. However, the Cl/OH reactivity ratio in Leicester is up to ≈ 9 times higher than that in Delhi. Cl reactivity is lower (Delhi: $\approx 685 \text{ s}^{-1}$, Leicester: $\approx 553 \text{ s}^{-1}$) during noontime and higher (Delhi: $\approx 750 \text{ s}^{-1}$, Leicester: $\approx 554 \text{ s}^{-1}$) during nighttime and early morning hours at both locations. The OH reactivity follows a similar pattern as that of Cl in Delhi and Leicester. The ratio of Cl to OH reactivity starts increasing after sunrise, 290 reaching a maximum value of ≈ 42 at nearly 16:00 h LT and then decreases further in Delhi. As mentioned above, Cl/OH reactivity ratio in Leicester shows a double peak pattern, with one peak (≈ 270) during early morning $\approx 04:00$ h LT and other peak (≈ 276) at about 16:00 h LT.

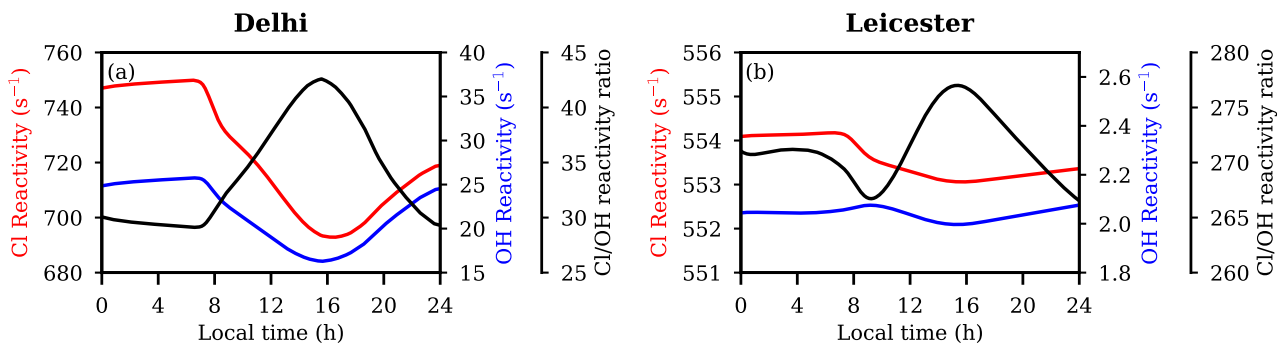


Figure 5. Reactivity of Cl and OH with CO, CH₄, and VOCs, and Cl/OH reactivity ratio during the simulation period in (a) Delhi and (b) Leicester.

We quantified the relative contribution of Cl in atmospheric oxidative capacity (AOC) using the model. AOC represents the 295 sum of oxidation rates of specie X_i by oxidants Y (OH, Cl, and other radicals: NO₃ and O₃) (Elshorbagy et al., 2009):

$$\text{AOC} = \sum k_{X_i} [X_i][Y] \quad (1)$$

where, k_{X_i} is the corresponding rate constant for X_i + Y reaction. Accordingly, the magnitude of AOC depends upon the concentration and reactivity of Cl. Figure 6 shows the contribution of individual oxidants in AOC at both locations. Besides OH, Cl is the second most important oxidant in Delhi, with a significant contribution of 23.4 % during morning (averaged 300 over 07:00-09:00 h LT), and 8.2 % throughout the day (06:00-16:00 h LT). In Leicester, Cl is the highest contributor (74.0 %) towards AOC during morning. In fact, with 34.1 % contribution, Cl is major oxidant after OH, during the daytime. The higher Besides the abundance of Cl, higher reactivity enhances the contribution of Cl in AOC, which is further substantiated by the ratio of Cl reactivity to OH reactivity (Fig. 5b). This ratio indicates that Cl reactivity exceeds OH reactivity by a significant

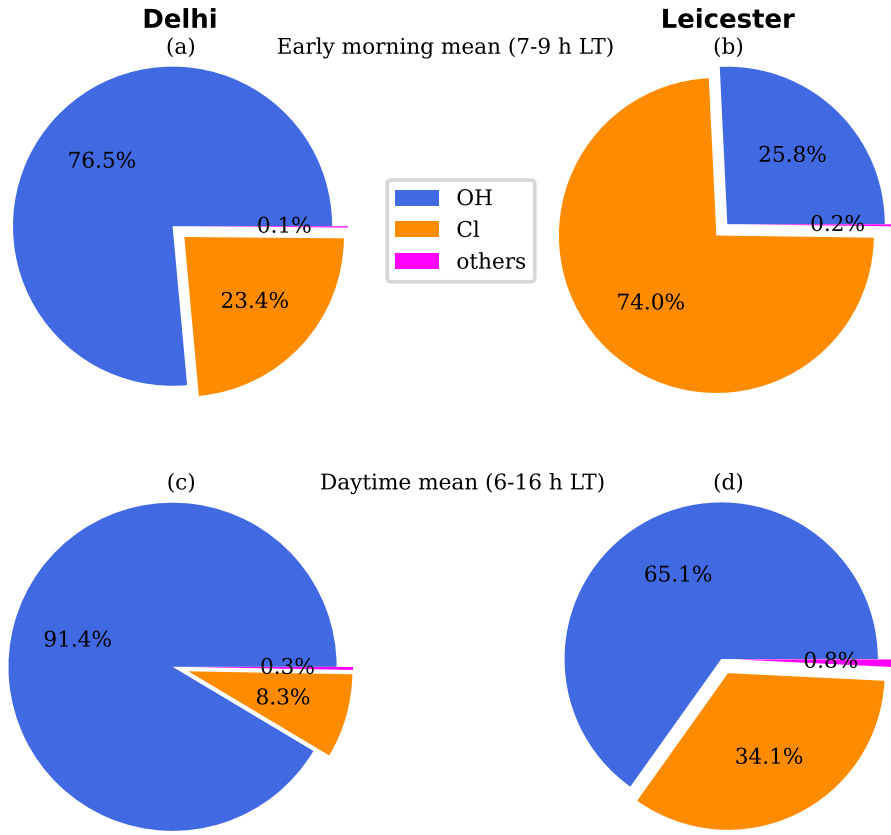


Figure 6. Atmospheric oxidative capacity (AOC) of radicals during (a, b) early morning mean (7-9 h LT) and (c, d) daytime mean (6-16 h LT) in Delhi (left panel) and Leicester (right panel).

margin, ranging from 265 to 276 times greater throughout the day in Leicester. Such a substantial contribution of Cl in AOC 305 leads to enhancements of RO_2 as seen in Fig. 3(f,l). Especially, a prominent peak in RO_2 during early morning (07:00-09:00 h LT) is imparted to strong participation of Cl in atmospheric oxidation during this time. Notably strongest contribution of Cl in AOC during early morning in Leicester, strengthens RO_2 peak by up to a factor of 8 (Fig. 3l). The role of Cl is predominant in Leicester as well as in Delhi during early morning, compared to a polluted environment of Hong Kong, China where Cl contribution was estimated to be 21.5 % (Xue et al., 2015). NO_3 and O_3 were found to play a relatively minor role in AOC at 310 both urban environments.

4.4 Sensitivity to $\text{ClNO}_2 + \text{Cl}^-$ reaction

In a study conducted by Haskins et al. (2019), using the reacto-diffusive length-scale framework, it was demonstrated that field and laboratory observations could be reconciled by considering an aqueous-phase reaction rate constant for the $\text{ClNO}_2 + \text{Cl}^-$ reaction on the order of $\approx 10^4 \text{ s}^{-1}$. This reaction rate constant is considerably lower (by ≈ 179 times) than reported in

315 Roberts et al. (2008). In this context, sensitivity simulation (NEWrate) is performed using a reaction rate coefficient of $5.6 \times 10^4 \text{ mol}^{-1} \text{ L s}^{-1}$ (Haskins et al., 2019) for the $\text{ClNO}_2 + \text{Cl}^-$ reaction, for both Delhi and Leicester. As depicted in Figure S7a, the concentration of Cl remains nearly the same in the NEWrate simulation compared to the NEW simulation over Delhi. However, there are significant changes in the concentration of ClNO_2 , as shown in Fig. S7b. The simulated ClNO_2 exhibits a broader peak and is approximately 30 pmol/mol higher near sunrise in the NEWrate simulation when compared to the NEW simulation. During the nighttime, approximately 20 pmol/mol of ClNO_2 is simulated in the NEWrate simulation, whereas it is negligible in the NEW simulation (see Fig. 3b). Since the Cl concentration is almost similar in both the NEW and NEWrate simulations, the differences in the simulated concentrations of OH, HO_2 , and RO_2 remain consistent between the NEWrate or NEW simulations and the OLD and NOCL simulations (refer to Fig. S7d, e, f, and Fig. 3d, e, f). The production and loss mechanisms of Cl are similar in both the NEW and NEWrate simulations (see Fig. S8a and Fig. 4a). The contributions 320 from ClNO_2 formation reactions are also similar. However, in contrast to the NEW simulation, the loss of ClNO_2 through photolysis becomes dominant and is ≈ 6 times greater than its loss through $\text{ClNO}_2 + \text{Cl}^-$ reaction, in NEWrate simulation. The contribution of radicals to AOC is also similar between the NEW and NEWrate simulation, as depicted in Fig. 6a,c and Fig. S9a,c respectively, over Delhi.

330 In contrast to Delhi, significant differences are seen in atmospheric composition in Leicester when the rate coefficient of the $\text{ClNO}_2 + \text{Cl}^-$ reaction is altered (as shown in Fig. S7). The peak concentration of Cl becomes $\approx 0.6 \text{ fmol/mol}$ during the morning hours of NEWrate simulation (Fig. S7g), which is about 4 times lower than the concentration of Cl in NEW simulation (Fig. 3g). However, due to slower rate of ClNO_2 consumption with Cl^- , the simulated ClNO_2 using the NEWrate is significantly enhanced (by ≈ 5 times) compared to NEW simulation, reaching a maximum of about 210 pmol/mol around 335 sunrise (see Fig. S7h). Due to lower Cl concentrations, the levels of ClONO also decrease by 3.5 times in NEWrate simulation (as shown in Fig. S7i) compared to NEW simulation (Fig. 3i). The dominant peak seen at sunrise in the NEW simulation for OH, HO_2 , and RO_2 is significantly reduced with the lower rate of the $\text{ClNO}_2 + \text{Cl}^-$ reaction, as illustrated in Fig S7j,k,l. Significant changes in the production and loss mechanisms of Cl and ClNO_2 are seen in Leicester when the reaction rate 340 of A6 is changed, as shown in Fig. S8 and Fig. 4b. For example, in the NEWrate simulation, other reactions, including the photolysis of ClNO_2 and ClONO , and $\text{ClO} + \text{NO}$ reaction, become prominent sources of Cl (with a rate of approximately $6.0 \times 10^5 \text{ molec cm}^{-3} \text{ s}^{-1}$), whereas in the NEW simulation, the major source for Cl is photolysis of Cl_2 . The primary source for ClNO_2 production remains the $\text{Cl}^- + \text{NO}_2^+$ reaction in both the NEW and NEWrate simulations. However, in the NEWrate simulation, ClNO_2 loss from photolysis becomes the major sink, whereas in the NEW simulation, loss from the $\text{ClNO}_2 + \text{Cl}^-$ reaction is prominent. In addition, remarkable changes in AOC are seen between the NEWrate (Fig. S9b, d) and the 345 NEW simulation (Fig. 6b,d). In the NEWrate simulation, even though Cl remains the major oxidant its contribution is notably reduced from 74% (in NEW simulation) to 58.1% during the early morning hours.

5 Summary and Conclusions

Extended gas- and aqueous-phase chemistry of chlorine compounds has been added to the MECCA mechanism. It consists of 36 gas-phase reactions (inorganic, organic, and photolysis reactions). A total of 24 aqueous-phase and heterogeneous reactions 350 have been added, containing detailed chemistry of N_2O_5 uptake on aerosols to yield ClNO_2 and various other competing reactions. The updated model is applied to two different urban environments: Delhi (India) and Leicester (United Kingdom) during winter time. The major conclusions are:

1. The model predicts up to 0.1 pmol/mol of NO_3 and up to 8 pmol/mol of N_2O_5 during daytime in Delhi. However, night-time production of NO_3 and N_2O_5 is seen to be negligible primarily due of the unavailability of O_3 . In contrast 355 to Delhi, NO_3 and N_2O_5 after mid-night in Leicester is ≈ 2.6 pmol/mol and ≈ 330 pmol/mol, respectively. N_2O_5 uptake on aerosols yields ClNO_2 , which produces Cl via photolysis.
2. A sharp build-up of Cl with sunrise is mainly through Cl_2 photolysis in Delhi. Besides Cl_2 , photolysis of ClNO_2 and ClONO and the reaction of ClO with NO are prominent Cl sources in Leicester. VOCs are the main sink for Cl at both 360 locations, whereas NO_2 is also an important sink for Cl in Leicester. The latter results in the formation of ClNO_2 with a major contribution in Delhi, while $\text{Cl}^- + \text{NO}_2^+$ is a stronger source in Leicester. Photolysis is the major sink for ClNO_2 in Delhi, however, its uptake on chloride aerosols is a prominent sink in Leicester.
3. The magnitude of Cl ($\approx 750 \text{ s}^{-1}$) and OH ($\approx 25 \text{ s}^{-1}$) reactivities are significantly greater in Delhi, particularly during the morning hours, when compared to Leicester. However, ~~pronounced~~ Cl to OH reactivity ratio (≈ 270) ~~of to reactivity in Leicester shows a much higher oxidation potential of compared to~~ is pronounced in Leicester coinciding with higher contribution of Cl in AOC. 365
4. Sensitivity simulations reveal substantial post-sunrise enhancements of in OH, HO_2 , and RO_2 radicals, with a prominent secondary peak due to Cl chemistry. Up to 8 times higher RO_2 is simulated in Leicester primarily because of leading role of Cl in AOC potential.

It is important to note that box models, despite their general limitation of neglecting transport phenomena and assuming species 370 to be well mixed, do include highly detailed chemical mechanisms. Furthermore, because the model is initialized with measurements of chemical species at both locations and the modeled levels align with observed data, significant discrepancies in model estimates would be unexpected. Future studies focussing on modeling vertical gradients, in particular for radical reservoir species such as HONO, and ClNO_2 (Young et al., 2012) are recommended.

375 This study highlights the vital role of Cl chemistry in governing the oxidation capacity of the atmosphere and air quality, and therefore it is important to account for it in detailed photochemical as well as in 3-D chemical transport models. This will lead to better ~~quantify~~ quantification of the importance of radicals in atmospheric oxidation and hence, the formation of ozone as well as secondary aerosols, over regional to global scale. Future studies focusing on secondary aerosol formation and new

particle formation from heterogeneous reactions are needed to deepen the understanding of transformation of trace gases to
380 aerosols.

Code and data availability. CAABA/MECCA is a community box model published under the GNU General Public Licence, available from the Gitlab repository (<https://gitlab.com/RolfSander/caaba-mecca>). The version of CAABA/MECCA updated in this study is currently available in the 'delhi' branch of the repository. The new chlorine mechanism will be included in the next release of CAABA/MECCA. All the model outputs associated with this study are archived at zenodo (<https://zenodo.org/record/8332131>; Soni et al. (2023)).

385 *Author contributions.* M. Soni, R. Sander, and D. Taraborrelli designed the study with inputs from S. S. Gunthe, P. Liu, and N. Ojha. M. Soni, R. Sander, and D. Taraborrelli developed and analyzed the chemical mechanism and M. Soni performed the simulations. A. Pozzer, R. Sander, L. K. Sahu, D. Taraborrelli, I. A. Girach, and N. Ojha helped M. Soni in the analyses and interpretations of the results. A. Patel assisted M. Soni in compiling literature and some input dataset. M. Soni wrote the manuscript and all the co-authors contributed to the review and editing.

390 *Competing interests.* At least one of the (co-)authors is a member of the editorial board of Atmospheric Chemistry and Physics.

495 *Acknowledgements.* The authors gratefully acknowledge the use of CAMS inventory for VOCs emissions data available from ECCAD (<https://eccad3.sedoo.fr/catalogue>). We thank ECMWF for the ERA5 dataset. We acknowledge UK AIR Air Information Resource for the chemical species data through <https://uk-air.defra.gov.uk/data/>. Authors thank J. M. Roberts (NOAA Chemical Sciences Laboratory, USA), Tao Wang (The Hong Kong Polytechnic University, Hong Kong), Men Xia (University of Helsinki, Finland), and Renuka Soni for valuable
395 inputs on kinetics. M. Soni, N. Ojha, and L. K. Sahu acknowledge support from the Physical Research Laboratory, Ahmedabad, funded by the Department of Space, Government of India.

References

Atkinson, R., Baulch, D. L., Cox, R. A., Crowley, J. N., Hampson, R. F., Hynes, R. G., Jenkin, M. E., Rossi, M. J., Troe, J., and IUPAC Subcommittee: Evaluated kinetic and photochemical data for atmospheric chemistry: Volume II – gas phase reactions of organic species, 400 Atmos. Chem. Phys., 6, 3625–4055, <https://doi.org/10.5194/ACP-6-3625-2006>, 2006.

Atkinson, R., Baulch, D. L., Cox, R. A., Crowley, J. N., Hampson, R. F., Hynes, R. G., Jenkin, M. E., Rossi, M. J., and Troe, J.: Evaluated kinetic and photochemical data for atmospheric chemistry: Volume III – gas phase reactions of inorganic halogens, Atmos. Chem. Phys., 7, 981–1191, <https://doi.org/10.5194/ACP-7-981-2007>, 2007.

Bannan, T. J., Booth, A. M., Bacak, A., Muller, J. B. A., Leather, K. E., Le Breton, M., Jones, B., Young, D., Coe, H., Allan, J., Visser, 405 Slowik, J. G., Furger, M., Prévôt, A. S. H., Lee, J., Dunmore, R. E., Hopkins, J. R., Hamilton, J. F., Lewis, A. C., Whalley, L. K., Sharp, T., Stone, D., Heard, D. E., Fleming, Z. L., Leigh, R., Shallcross, D. E., and Percival, C. J.: The first UK measurements of nitryl chloride using a chemical ionization mass spectrometer in central London in the summer of 2012, and an investigation of the role of Cl atom oxidation, Journal of Geophysical Research: Atmospheres, 120, 5638–5657, <https://doi.org/https://doi.org/10.1002/2014JD022629>, 2015.

410 Behnke, W., George, C., Scheer, V., and Zetzsch, C.: Production and decay of ClNO₂ from the reaction of gaseous N₂O₅ with NaCl solution: Bulk and aerosol experiments, J. Geophys. Res., 102D, 3795–3804, <https://doi.org/10.1029/96JD03057>, 1997.

Bertram, T. H. and Thornton, J. A.: Toward a general parameterization of N₂O₅ reactivity on aqueous particles: the competing effects of 415 particle liquid water, nitrate and chloride, Atmos. Chem. Phys., 9, 8351–8363, <https://doi.org/10.5194/ACP-9-8351-2009>, 2009.

Brown, S., Stark, H., Ciciora, S., and Ravishankara, A.: In-situ Measurement of Atmospheric NO₃ and N₂O₅ via Cavity Ring-down Spectroscopy, Geophysical Research Letters - GEOPHYS RES LETT, 28, 3227–3230, <https://doi.org/10.1029/2001GL013303>, 2001.

420 Brown, S. S., Osthoff, H. D., Stark, H., Dubé, W. P., Ryerson, T. B., Warneke, C., de Gouw, J. A., Wollny, A. G., Parrish, D. D., Fehsenfeld, F. C., and Ravishankara, A.: Aircraft observations of daytime NO₃ and N₂O₅ and their implications for tropospheric chemistry, Journal of Photochemistry and Photobiology A: Chemistry, 176, 270–278, <https://doi.org/https://doi.org/10.1016/j.jphotochem.2005.10.004>, in Honour of Professor Richard P. Wayne, 2005.

Burkholder, J. B., Sander, S. P., Abbatt, J., Barker, J. R., Huie, R. E., Kolb, C. E., Kurylo, M. J., Orkin, V. L., Wilmouth, D. M., and 425 Wine, P. H.: Chemical Kinetics and Photochemical Data for Use in Atmospheric Studies, Evaluation No. 18, JPL Publication 15-10, Jet Propulsion Laboratory, Pasadena, <http://jpldataeval.jpl.nasa.gov>, 2015.

Chen, Y., Beig, G., Archer-Nicholls, S., Drysdale, W., Acton, W. J. F., Lowe, D., Nelson, B., Lee, J., Ran, L., Wang, Y., Wu, Z., Sahu, S. K., 430 Sokhi, R. S., Singh, V., Gadi, R., Nicholas Hewitt, C., Nemitz, E., Archibald, A., McFiggans, G., and Wild, O.: Avoiding high ozone pollution in Delhi, India, Faraday Discuss., 226, 502–514, <https://doi.org/10.1039/D0FD00079E>, 2021.

Choi, M. S., Qiu, X., Zhang, J., Wang, S., Li, X., Sun, Y., Chen, J., and Ying, Q.: Study of Secondary Organic Aerosol Formation from Chlorine Radical-Initiated Oxidation of Volatile Organic Compounds in a Polluted Atmosphere Using a 3D Chemical Transport Model, Environmental Science & Technology, 54, 13 409–13 418, <https://doi.org/10.1021/acs.est.0c02958>, pMID: 33074656, 2020.

Coombes, R. G., Golding, J. G., and Hadjigeorgiou, P.: Electrophilic aromatic substitution. Part 23. The nitration of phenol and the cresols in aqueous sulphuric acid, J. Chem. Soc. Perkin Trans. 2, pp. 1451–1459, <https://doi.org/10.1039/P29790001451>, 1979.

Elshorbany, Y. F., Kurtenbach, R., Wiesen, P., Lissi, E., Rubio, M., Villena, G., Gramsch, E., Rickard, A. R., Pilling, M. J., and Kleffmann, J.: Oxidation capacity of the city air of Santiago, Chile, Atmospheric Chemistry and Physics, 9, 2257–2273, <https://doi.org/10.5194/acp-9-2257-2009>, 2009.

Fan, J. and Zhang, R.: Atmospheric Oxidation Mechanism of Isoprene, *Environ. Chem.*, 1, 140–149, <https://doi.org/10.1071/EN04045>, 2004.

435 Faxon, C. and Allen, D.: Chlorine chemistry in urban atmospheres: A review, *Environmental Chemistry*, 10, 221–233, <https://doi.org/10.1071/EN13026>, 2013.

Fickert, S., Helleis, F., Adams, J. W., Moortgat, G. K., and Crowley, J. N.: Reactive uptake of ClNO₂ on aqueous bromide solutions, *J. Phys. Chem. A*, 102, 10 689–10 696, <https://doi.org/10.1021/JP983004N>, 1998.

Frenzel, A., Scheer, V., Sikorski, R., C., G., Behnke, W., and Zetzsch, C.: Heterogeneous interconversion reactions of BrNO₂, ClNO₂, Br₂, and Cl₂, *J. Phys. Chem. A*, 102, 1329–1337, <https://doi.org/10.1021/JP973044B>, 1998.

440 Fried, A., Henry, B. E., Calvert, J. G., and M., M.: The reaction probability of N₂O₅ with sulfuric acid aerosols at stratospheric temperatures and compositions, *J. Geophys. Res.*, 99D, 3517–3532, <https://doi.org/10.1029/93JD01907>, 1994.

Geyer, A., Aliche, B., Ackermann, R., Martinez, M., Harder, H., Brune, W., di Carlo, P., Williams, E., Jobson, T., Hall, S., Shetter, R., and Stutz, J.: Direct observations of daytime NO₃: Implications for urban boundary layer chemistry, *Journal of Geophysical Research: Atmospheres*, 108, 4368, <https://doi.org/https://doi.org/10.1029/2002JD002967>, 2003.

445 Ghosh, B., Papanastasiou, D. K., Talukdar, R. K., Roberts, J. M., and Burkholder, J. B.: Nitryl Chloride (ClNO₂): UV/Vis Absorption Spectrum between 210 and 296 K and O(3P) Quantum Yield at 193 and 248 nm, *The Journal of Physical Chemistry A*, 116, 5796–5805, <https://doi.org/10.1021/jp207389y>, pMID: 21936506, 2012.

Golden, D. M.: The Reaction Cl + NO₂ → ClONO and ClNO₂, *The Journal of Physical Chemistry A*, 111, 6772–6780, <https://doi.org/10.1021/jp069000x>, pMID: 17547376, 2007.

450 Granier, C., Darras, S., van der Gon, H. D., Doubalova, J., Elguindi, N., Galle, B., Gauss, M., Guevara, M., Jalkanen, J.-P., Kuenen, J., Liouesse, C., Quack, B., Simpson, D., and Sindelarova, K.: The Copernicus Atmosphere Monitoring Service global and regional emissions (April 2019 version), Copernicus Atmosphere Monitoring Service (CAMS) report, <https://doi.org/10.24380/d0bn-kx16>, 2019.

Green, M., Yarwood, G., and Niki, H.: FTIR study of the Cl-atom initiated oxidation of methylglyoxal, *Int. J. Chem. Kinet.*, 22, 689–699, <https://doi.org/10.1002/KIN.550220705>, 1990.

455 Grigorev, A. E., Makarov, I. E., and Pikaev, A. K.: Formation of Cl₂⁻ in the bulk solution during the radiolysis of concentrated aqueous solutions of chlorides, *High Energy Chem.*, 21, 99–102, <https://kinetics.nist.gov/solution/Detail?id=1987GRI/MAK99-102:2>, 1987.

Gunthe, S., Liu, P., Panda, U., S Raj, S., Sharma, A., Darbyshire, E., Reyes Villegas, E., Allan, J., Chen, Y., Wang, X., Song, S., Pohlker, M., Shi, L., Wang, Y., Kommula, S., Liu, T., Ravikrishna, R., McFiggans, G., Mickley, L., and Coe, H.: Enhanced aerosol particle growth sustained by high continental chlorine emission in India, *Nature Geoscience*, 14, <https://doi.org/10.1038/s41561-020-00677-x>, 2021.

460 Haskins, J. D., Lee, B. H., Lopez-Hilfiker, F. D., Peng, Q., Jaeglé, L., Reeves, J. M., Schroder, J. C., Campuzano-Jost, P., Fibiger, D., McDuffie, E. E., Jiménez, J. L., Brown, S. S., and Thornton, J. A.: Observational Constraints on the Formation of Cl₂ From the Reactive Uptake of ClNO₂ on Aerosols in the Polluted Marine Boundary Layer, *Journal of Geophysical Research: Atmospheres*, 124, 8851–8869, <https://doi.org/https://doi.org/10.1029/2019JD030627>, 2019.

Haslett, S. L., Bell, D. M., Kumar, V., Slowik, J. G., Wang, D. S., Mishra, S., Rastogi, N., Singh, A., Ganguly, D., Thornton, J., Zheng, F., Li, Y., Nie, W., Liu, Y., Ma, W., Yan, C., Kulmala, M., Daellenbach, K. R., Hadden, D., Baltensperger, U., Prevot, A. S. H., Tripathi, S. N., and Mohr, C.: Nighttime NO emissions strongly suppress chlorine and nitrate radical formation during the winter in Delhi, *Atmospheric Chemistry and Physics*, 23, 9023–9036, <https://doi.org/10.5194/acp-23-9023-2023>, 2023.

465 Heal, M. R., Harrison, M. A. J., and Cape, J. N.: Aqueous-phase nitration of phenol by N₂O₅ and ClNO₂, *Atmos. Environ.*, 41, 3515–3520, <https://doi.org/10.1016/J.ATMOSENV.2007.02.003>, 2007.

470

Hens, K., Novelli, A., Martinez, M., Auld, J., Axinte, R., Bohn, B., Fischer, H., Keronen, P., Kubistin, D., Nölscher, A. C., Oswald, R., Paasonen, P., Petäjä, T., Regelin, E., Sander, R., Sinha, V., Sipilä, M., Taraborrelli, D., Tatum Ernest, C., Williams, J., Lelieveld, J., and Harder, H.: Observation and modelling of HO_x radicals in a boreal forest, *Atmospheric Chemistry and Physics*, 14, 8723–8747, <https://doi.org/10.5194/acp-14-8723-2014>, 2014.

475 Hersbach, H., Bell, B., Berrisford, P., Hirahara, S., Horányi, A., Muñoz-Sabater, J., Nicolas, J., Peubey, C., Radu, R., Schepers, D., Simmonds, A., Soci, C., Abdalla, S., Abellán, X., Balsamo, G., Bechtold, P., Biavati, G., Bidlot, J., Bonavita, M., De Chiara, G., Dahlgren, P., Dee, D., Diamantakis, M., Dragani, R., Flemming, J., Forbes, R., Fuentes, M., Geer, A., Haimberger, L., Healy, S., Hogan, R. J., Hólm, E., Janisková, M., Keeley, S., Laloyaux, P., Lopez, P., Lupu, C., Radnoti, G., de Rosnay, P., Rozum, I., Vamborg, F., Villaume, S., and Thépaut, J.-N.: The ERA5 global reanalysis, *Quarterly Journal of the Royal Meteorological Society*, 146, 1999–2049, [https://doi.org/https://doi.org/10.1002/qj.3803](https://doi.org/10.1002/qj.3803), 2020.

480 Horowitz, L. W., Fiore, A. M., Milly, G. P., Cohen, R. C., Perring, A., Wooldridge, P. J., Hess, P. G., Emmons, L. K., and Lamarque, J.-F.: Observational constraints on the chemistry of isoprene nitrates over the eastern United States, *Journal of Geophysical Research: Atmospheres*, 112, [https://doi.org/https://doi.org/10.1029/2006JD007747](https://doi.org/10.1029/2006JD007747), 2007.

485 Hossaini, R., Chipperfield, M. P., Saiz-Lopez, A., Fernandez, R., Monks, S., Feng, W., Brauer, P., and von Glasow, R.: A global model of tropospheric chlorine chemistry: Organic versus inorganic sources and impact on methane oxidation, *Journal of Geophysical Research: Atmospheres*, 121, 14,271–14,297, [https://doi.org/https://doi.org/10.1002/2016JD025756](https://doi.org/10.1002/2016JD025756), 2016.

490 Iraci, L. T., Riffel, B. G., Robinson, C. B., Michelsen, R. R., and Stephenson, R. M.: The acid catalyzed nitration of methanol: formation of methyl nitrate via aerosol chemistry, *J. Atmos. Chem.*, 58, 253–266, <https://doi.org/10.1007/S10874-007-9091-9>, 2007.

Janowski, B., Knauth, H.-D., and Martin, H.: Chlornitrit, ein metastabiles Zwischenprodukt der Reaktion von 495 Dichlormonoxid mit Nitrosylchlorid, *Berichte der Bunsengesellschaft für physikalische Chemie*, 81, 1262–1270, [https://doi.org/https://doi.org/10.1002/bbpc.19770811212](https://doi.org/10.1002/bbpc.19770811212), 1977.

Khan, A., Morris, W., Watson, L., Galloway, M., Hamer, P., Shallcross, B., Percival, C., and Shallcross, D.: Estimation of Daytime NO₃ Radical Levels in the UK Urban Atmosphere Using the Steady State Approximation Method, *Advances in Meteorology*, 2015, 9, <https://doi.org/10.1155/2015/294069>, 2015a.

495 Khan, M., Cooke, M., Utembe, S., Archibald, A., Derwent, R., Xiao, P., Percival, C., Jenkin, M., Morris, W., and Shallcross, D.: Global modeling of the nitrate radical (NO₃) for present and pre-industrial scenarios, *Atmospheric Research*, 164–165, 347–357, <https://doi.org/https://doi.org/10.1016/j.atmosres.2015.06.006>, 2015b.

500 Knipping, E. M., Lakin, M. J., Foster, K. L., Jungwirth, P., Tobias, D. J., Gerber, R. B., Dabdub, D., and Finlayson-Pitts, B. J.: Experiments and simulations of ion-enhanced interfacial chemistry on aqueous NaCl aerosols, *Science*, 288, 301–306, <https://doi.org/10.1126/SCIENCE.288.5464.301>, 2000.

Kroflič, A., Grilc, M., and Grgić, I.: Unraveling Pathways of Guaiacol Nitration in Atmospheric Waters: Nitrite, A Source of Reactive Nitronium Ion in the Atmosphere, *Environmental Science & Technology*, 49, 9150–9158, <https://doi.org/10.1021/acs.est.5b01811>, pMID: 26162010, 2015.

Landgraf, J. and Crutzen, P. J.: An efficient method for online calculations of photolysis and heating rates, *J. Atmos. Sci.*, 55, 863–878, [https://doi.org/10.1175/1520-0469\(1998\)055<0863:AEMFOC>2.0.CO;2](https://doi.org/10.1175/1520-0469(1998)055<0863:AEMFOC>2.0.CO;2), 1998.

505 Lanz, V. A., Prévôt, A. S. H., Alfarra, M. R., Weimer, S., Mohr, C., DeCarlo, P. F., Gianini, M. F. D., Hueglin, C., Schneider, J., Favez, O., D'Anna, B., George, C., and Baltensperger, U.: Characterization of aerosol chemical composition with aerosol mass spectrometry in Central Europe: an overview, *Atmospheric Chemistry and Physics*, 10, 10 453–10 471, <https://doi.org/10.5194/acp-10-10453-2010>, 2010.

Lawler, M. J., Sander, R., Carpenter, L. J., Lee, J. D., von Glasow, R., Sommariva, R., and Saltzman, E. S.: HOCl and Cl₂ observations in marine air, *Atmospheric Chemistry and Physics*, 11, 7617–7628, <https://doi.org/10.5194/acp-11-7617-2011>, 2011.

510 Liao, J., Huey, L., Liu, Z., Tanner, D., Cantrell, C., Orlando, J., Flocke, F., Shepson, P., Weinheimer, A., Hall, S., Ullmann, K., Beine, H., Wang, Y., Ingall, E., Stephens, C., Hornbrook, R., Apel, E., Riemer, D., Fried, A., and Nowak, J.: High levels of molecular chlorine in the Arctic atmosphere, *Nature Geoscience*, 7, <https://doi.org/10.1038/ngeo2046>, 2014.

515 Liu, X., Qu, H., Huey, L. G., Wang, Y., Sjostedt, S., Zeng, L., Lu, K., Wu, Y., Hu, M., Shao, M., Zhu, T., and Zhang, Y.: High Levels of Daytime Molecular Chlorine and Nitryl Chloride at a Rural Site on the North China Plain, *Environmental Science & Technology*, 51, 9588–9595, <https://doi.org/10.1021/acs.est.7b03039>, pMID: 28806070, 2017.

Lobert, J. M., Keene, W. C., Logan, J. A., and Yevich, R.: Global chlorine emissions from biomass burning: Reactive Chlorine Emissions Inventory, *Journal of Geophysical Research: Atmospheres*, 104, 8373–8389, <https://doi.org/https://doi.org/10.1029/1998JD100077>, 1999.

Müller, B. and Heal, M. R.: The Henry's law coefficient of 2-nitrophenol over the temperature range 278–303 K, *Chemosphere*, 45, 309–314, 520 [https://doi.org/10.1016/S0045-6535\(00\)00592-0](https://doi.org/10.1016/S0045-6535(00)00592-0), 2001.

Nakoudi, K., Giannakaki, E., Dandou, A., Tombrou, M., and Komppula, M.: Planetary Boundary Layer variability over New Delhi, India, during EUCAARI project, *Atmospheric Measurement Techniques Discussions*, pp. 1–33, <https://doi.org/10.5194/amt-2018-342>, 2018.

Nelson, B. S., Stewart, G. J., Drysdale, W. S., Newland, M. J., Vaughan, A. R., Dunmore, R. E., Edwards, P. M., Lewis, A. C., Hamilton, J. F., Acton, W. J., Hewitt, C. N., Crilley, L. R., Alam, M. S., Şahin, U. A., Beddows, D. C. S., Bloss, W. J., Slater, E., Whalley, L. K., 525 Heard, D. E., Cash, J. M., Langford, B., Nemitz, E., Sommariva, R., Cox, S., Shivani, Gadi, R., Gurjar, B. R., Hopkins, J. R., Rickard, A. R., and Lee, J. D.: In situ ozone production is highly sensitive to volatile organic compounds in Delhi, India, *Atmospheric Chemistry and Physics*, 21, 13 609–13 630, <https://doi.org/10.5194/acp-21-13609-2021>, 2021.

Nelson, B. S., Bryant, D. J., Alam, M. S., Sommariva, R., Bloss, W. J., Newland, M. J., Drysdale, W. S., Vaughan, A. R., Acton, W. J. F., 530 Hewitt, C. N., Crilley, L. R., Swift, S. J., Edwards, P. M., Lewis, A. C., Langford, B., Nemitz, E., Shivani, Gadi, R., Gurjar, B. R., Heard, D. E., Whalley, L. K., Sahin, U. A., Beddows, D. C. S., Hopkins, J. R., Lee, J. D., Rickard, A. R., and Hamilton, J. F.: Extreme Concentrations of Nitric Oxide Control Daytime Oxidation and Quench Nocturnal Oxidation Chemistry in Delhi during Highly Polluted Episodes, *Environmental Science & Technology Letters*, 10, 520–527, <https://doi.org/10.1021/acs.estlett.3c00171>, 2023.

Niki, H., Maker, P., Savage, C., and Breitenbach, L.: Fourier transform IR spectroscopic observation of chlorine nitrite, ciono, formed via Cl + NO₂ (+M) → ClONO(+M), *Chemical Physics Letters*, 59, 78–79, [https://doi.org/https://doi.org/10.1016/0009-2614\(78\)85618-8](https://doi.org/https://doi.org/10.1016/0009-2614(78)85618-8), 1978.

535 Niki, H., Maker, P. D., Savage, C. M., and Breitenbach, L. P.: An FTIR study of the Cl-atom-initiated reaction of glyoxal, *Int. J. Chem. Kinet.*, 17, 547–558, <https://doi.org/10.1002/KIN.550170507>, 1985.

Niki, H., Maker, P. D., Savage, C. M., and Hurley, M. D.: Fourier transform infrared study of the kinetics and mechanisms for the Cl-atom- and HO-radical-initiated oxidation of glycolaldehyde, *J. Phys. Chem.*, 91, 2174–2178, <https://doi.org/10.1021/J100292A038>, 1987.

Nölscher, A., Butler, T., Auld, J., Veres, P., Muñoz, A., Taraborrelli, D., Vereecken, L., Lelieveld, J., and Williams, J.: Using total OH reactivity to assess isoprene photooxidation via measurement and model, *Atmospheric Environment*, 89, 453–463, 540 <https://doi.org/https://doi.org/10.1016/j.atmosenv.2014.02.024>, 2014.

Osthoff, H. D., Roberts, J. M., Ravishankara, A. R., Williams, E. J., Lerner, B. M., Sommariva, R., Bates, T. S., Coffman, D., Quinn, P. K., Dibb, J. E., Stark, H., Burkholder, J. B., Talukdar, R. K., Meagher, J., Fehsenfeld, F. C., and Brown, S. S.: High levels of nitryl chloride in the polluted subtropical marine boundary layer, *Nature Geosci.*, 1, 324–328, <https://doi.org/10.1038/NGEO177>, 2008.

545 Pawar, P. V., Ghude, S. D., Govardhan, G., Acharja, P., Kulkarni, R., Kumar, R., Sinha, B., Sinha, V., Jena, C., Gunwani, P., Adhya, T. K., Nemitz, E., and Sutton, M. A.: Chloride (HCl / Cl⁻) dominates inorganic aerosol formation from ammonia in the Indo-Gangetic Plain

during winter: modeling and comparison with observations, *Atmospheric Chemistry and Physics*, 23, 41–59, <https://doi.org/10.5194/acp-23-41-2023>, 2023.

550 Pozzer, A., Reifenberg, S. F., Kumar, V., Franco, B., Kohl, M., Taraborrelli, D., Gromov, S., Ehrhart, S., Jöckel, P., Sander, R., Fall, V., Rosanka, S., Karydis, V., Akritudis, D., Emmerichs, T., Crippa, M., Guizzardi, D., Kaiser, J. W., Clarisse, L., Kiendler-Scharr, A., Tost, H., and Tsimpidi, A.: Simulation of organics in the atmosphere: evaluation of EMACv2.54 with the Mainz Organic Mechanism (MOM) coupled to the ORACLE (v1.0) submodel, *Geoscientific Model Development*, 15, 2673–2710, <https://doi.org/10.5194/gmd-15-2673-2022>, 2022.

555 Qiu, X., Ying, Q., Wang, S., Duan, L., Wang, Y., Lu, K., Wang, P., Xing, J., Zheng, M., Zhao, M., Zheng, H., Zhang, Y., and Hao, J.: Significant impact of heterogeneous reactions of reactive chlorine species on summertime atmospheric ozone and free-radical formation in north China, *Sci. Total Environ.*, 693, 133 580, <https://doi.org/10.1016/J.SCITOTENV.2019.133580>, 2019a.

Qiu, X., Ying, Q., Wang, S., Duan, L., Zhao, J., Xing, J., Ding, D., Sun, Y., Liu, B., Shi, A., Yan, X., Xu, Q., and Hao, J.: Modeling the impact of heterogeneous reactions of chlorine on summertime nitrate formation in Beijing, China, *Atmospheric Chemistry and Physics*, 19, 6737–6747, <https://doi.org/10.5194/acp-19-6737-2019>, 2019b.

560 Ragains, M. L. and Finlayson-Pitts, B. J.: Kinetics and Mechanism of the Reaction of Cl Atoms with 2-Methyl-1,3-butadiene (Isoprene) at 298 K, *The Journal of Physical Chemistry A*, 101, 1509–1517, <https://doi.org/10.1021/jp962786m>, 1997.

Ravishankara, A. R.: Are chlorine atoms significant tropospheric free radicals?, *Proceedings of the National Academy of Sciences*, 106, 13 639–13 640, <https://doi.org/10.1073/pnas.0907089106>, 2009.

Rickard, A.: Master Chemical Mechanism, MCM v3.3.1, <http://mcm.york.ac.uk>, 2009.

565 Riedel, T. P., Wolfe, G. M., Danas, K. T., Gilman, J. B., Kuster, W. C., Bon, D. M., Vlasenko, A., Li, S.-M., Williams, E. J., Lerner, B. M., Veres, P. R., Roberts, J. M., Holloway, J. S., Lefer, B., Brown, S. S., and Thornton, J. A.: An MCM modeling study of nitryl chloride (ClNO₂) impacts on oxidation, ozone production and nitrogen oxide partitioning in polluted continental outflow, *Atmospheric Chemistry and Physics*, 14, 3789–3800, <https://doi.org/10.5194/acp-14-3789-2014>, 2014.

Roberts, J. M., Osthoff, H. D., Brown, S. S., and Ravishankara, A. R.: N₂O₅ oxidizes chloride to Cl₂ in acidic atmospheric aerosol, *Science*, 570 321, 1059, <https://doi.org/10.1126/SCIENCE.1158777>, 2008.

Roberts, J. M., Osthoff, H. D., Brown, S. S., Ravishankara, A. R., Coffman, D., Quinn, P., and Bates, T.: Laboratory studies of products of N₂O₅ uptake on Cl-containing substrates, *Geophysical Research Letters*, 36, <https://doi.org/10.1029/2009GL040448>, 2009.

Rosanka, S., Sander, R., Wahner, A., and Taraborrelli, D.: Oxidation of low-molecular-weight organic compounds in cloud droplets: development of the Jülich Aqueous-phase Mechanism of Organic Chemistry (JAMOC) in CAABA/MECCA (version 4.5.0), *Geoscientific Model Development*, 14, 4103–4115, <https://doi.org/10.5194/gmd-14-4103-2021>, 2021.

Ryder, O. S., Campbell, N. R., Shaloski, M., Al-Mashat, H., Nathanson, G. M., and Bertram, T. H.: Role of organics in regulating ClNO₂ production at the air-sea interface, *J. Phys. Chem. A*, 119, 8519–8526, <https://doi.org/10.1021/JP5129673>, 2015.

Saiz-Lopez, A. and von Glasow, R.: Reactive halogen chemistry in the troposphere, *Chem. Soc. Rev.*, 41, 6448–6472, 580 <https://doi.org/10.1039/C2CS35208G>, 2012.

Sander, R.: Compilation of Henry's law constants (version 4.0) for water as solvent, *Atmos. Chem. Phys.*, 15, 4399–4981, <https://doi.org/10.5194/ACP-15-4399-2015>, 2015.

585 Sander, R., Jöckel, P., Kirner, O., Kunert, A. T., Landgraf, J., and Pozzer, A.: The photolysis module JVAL-14, compatible with the MESSY standard, and the JVal PreProcessor (JVPP), *Geoscientific Model Development*, 7, 2653–2662, <https://doi.org/10.5194/gmd-7-2653-2014>, 2014.

590 Sander, R., Baumgaertner, A., Cabrera-Perez, D., Frank, F., Gromov, S., Groß, J.-U., Harder, H., Huijnen, V., Jöckel, P., Karydis, V. A., Niemeyer, K. E., Pozzer, A., Riede, H., Schultz, M. G., Taraborrelli, D., and Tauer, S.: The community atmospheric chemistry box model CAABA/MECCA-4.0, *Geoscientific Model Development*, 12, 1365–1385, <https://doi.org/10.5194/gmd-12-1365-2019>, 2019.

595 Sandu, A. and Sander, R.: Technical note: Simulating chemical systems in Fortran90 and Matlab with the Kinetic PreProcessor KPP-2.1, *Atmos. Chem. Phys.*, 6, 187–195, <https://doi.org/10.5194/ACP-6-187-2006>, 2006.

Sapoli, M., De Santis, A., Marziano, N. C., Pinna, F., and Zingales, A.: Equilibria of nitric acid in sulfuric and perchloric acid at 25.degree.C by Raman and UV spectroscopy, *The Journal of Physical Chemistry*, 89, 2864–2869, <https://doi.org/10.1021/j100259a032>, 1985.

600 Sarwar, G., Simon, H., Xing, J., and Mathur, R.: Importance of tropospheric ClNO₂ chemistry across the Northern Hemisphere, *Geophysical Research Letters*, 41, 4050–4058, [https://doi.org/https://doi.org/10.1002/2014GL059962](https://doi.org/10.1002/2014GL059962), 2014.

605 Seinfeld, J. H. and Pandis, S. N.: *Atmospheric Chemistry and Physics*, John Wiley & Sons, Inc., 2016.

Sharma, G., Sinha, B., Pallavi, Hakkim, H., Chandra, B. P., Kumar, A., and Sinha, V.: Gridded Emissions of CO, NO_x, SO₂, CO₂, NH₃, HCl, CH₄, PM2.5, PM10, BC, and NMVOC from Open Municipal Waste Burning in India, *Environmental Science & Technology*, 53, 4765–4774, <https://doi.org/10.1021/acs.est.8b07076>, 2019.

610 Shi, J. and Bernhard, M. J.: Kinetic studies of Cl-atom reactions with selected aromatic compounds using the photochemical reactor-FTIR spectroscopy technique, *Int. J. Chem. Kinet.*, 29, 349–358, [https://doi.org/10.1002/\(SICI\)1097-4601\(1997\)29:5<349::AID-KIN5>3.0.CO;2-U](https://doi.org/10.1002/(SICI)1097-4601(1997)29:5<349::AID-KIN5>3.0.CO;2-U), 1997.

Sindelarova, K., Granier, C., Bouarar, I., Guenther, A., Tilmes, S., Stavrakou, T., Müller, J.-F., Kuhn, U., Stefani, P., and Knorr, W.: Global data set of biogenic VOC emissions calculated by the MEGAN model over the last 30 years, *Atmospheric Chemistry and Physics*, 14, 9317–9341, <https://doi.org/10.5194/acp-14-9317-2014>, 2014.

615 Sokolov, O., Hurley, M. D., Ball, J. C., Wallington, T. J., Nelsen, W., Barnes, I., and Becker, K. H.: Kinetics of the reactions of chlorine atoms with CH₃ONO and CH₃ONO₂, *Int. J. Chem. Kinet.*, 31, 357–359, [https://doi.org/10.1002/\(SICI\)1097-4601\(1999\)31:5<357::AID-KIN5>3.0.CO;2-6](https://doi.org/10.1002/(SICI)1097-4601(1999)31:5<357::AID-KIN5>3.0.CO;2-6), 1999.

620 Sommariva, R., Hollis, L. D. J., Sherwen, T., Baker, A. R., Ball, S. M., Bandy, B. J., Bell, T. G., Chowdhury, M. N., Cordell, R. L., Evans, M. J., Lee, J. D., Reed, C., Reeves, C. E., Roberts, J. M., Yang, M., and Monks, P. S.: Seasonal and geographical variability of nitryl chloride and its precursors in Northern Europe, *Atmospheric Science Letters*, 19, e844, [https://doi.org/https://doi.org/10.1002/asl.844](https://doi.org/10.1002/asl.844), 2018.

Sommariva, R., Crilley, L. R., Ball, S. M., Cordell, R. L., Hollis, L. D., Bloss, W. J., and Monks, P. S.: Enhanced wintertime oxidation of VOCs via sustained radical sources in the urban atmosphere, *Environmental Pollution*, 274, 116563, <https://doi.org/https://doi.org/10.1016/j.envpol.2021.116563>, 2021.

625 Soni, M., Sander, R., Taraborrelli, D., and Ojha, N.: Model outputs associated with "Comprehensive multiphase chlorine chemistry in the box model CAABA/MECCA: Implications to atmospheric oxidative capacity" [Data set], Zenodo, <https://doi.org/10.5281/zenodo.8332131>, 2023.

630 Staudt, S., Gord, J. R., Karimova, N. V., McDuffie, E. E., Brown, S. S., Gerber, R. B., Nathanson, G. M., and Bertram, T. H.: Sulfate and carboxylate suppress the formation of ClNO₂ at atmospheric interfaces, *Earth Space Chem.*, 3, 1987–1997, <https://doi.org/10.1021/ACSEARTHSPACECHEM.9B00177>, 2019.

Taraborrelli, D., Lawrence, M. G., Crowley, J. N., Dillon, T. J., Gromov, S., Groß, C. B. M., Vereecken, L., and Lelieveld, J.: Hydroxyl radical buffered by isoprene oxidation over tropical forests, *Nature Geosci.*, 5, 190–193, <https://doi.org/10.1038/NGEO1405>, 2012.

Taraborrelli, D., Cabrera-Perez, D., Bacer, S., Gromov, S., Lelieveld, J., Sander, R., and Pozzer, A.: Influence of aromatics on tropospheric gas-phase composition, *Atmospheric Chemistry and Physics*, 21, 2615–2636, <https://doi.org/10.5194/acp-21-2615-2021>, 2021.

625 Tham, Y. J., Wang, Z., Li, Q., Yun, H., Wang, W., Wang, X., Xue, L., Lu, K., Ma, N., Bohn, B., Li, X., Kecorius, S., Größ, J., Shao, M., Wiedensohler, A., Zhang, Y., and Wang, T.: Significant concentrations of nitryl chloride sustained in the morning: investigations of the causes and impacts on ozone production in a polluted region of northern China, *Atmospheric Chemistry and Physics*, 16, 14 959–14 977, <https://doi.org/10.5194/acp-16-14959-2016>, 2016.

630 Thiault, G., Mellouki, A., and Bras, G. L.: Kinetics of gas phase reactions of OH and Cl with aromatic aldehydes, *Phys. Chem. Chem. Phys.*, 4, 2194–2199, <https://doi.org/10.1039/b200609j>, 2002.

Thornton, J., Kercher, J., Riedel, T., Wagner, N., Cozic, J., Holloway, J., Dubé, W., Wolfe, G., Quinn, P., Middlebrook, A., Alexander, B., and Brown, S.: A large atomic chlorine source inferred from mid-continental reactive nitrogen chemistry, *Nature*, 464, 271–4, <https://doi.org/10.1038/nature08905>, 2010.

635 Tripathi, N., Sahu, L. K., Wang, L., Vats, P., Soni, M., Kumar, P., Satish, R. V., Bhattu, D., Sahu, R., Patel, K., Rai, P., Kumar, V., Rastogi, N., Ojha, N., Tiwari, S., Ganguly, D., Slowik, J., Prévôt, A. S. H., and Tripathi, S. N.: Characteristics of VOC Composition at Urban and Suburban Sites of New Delhi, India in Winter, *Journal of Geophysical Research: Atmospheres*, 127, e2021JD035342, <https://doi.org/https://doi.org/10.1029/2021JD035342>, 2021JD035342, 2022.

von Glasow, R. and Crutzen, P.: Tropospheric Halogen Chemistry, in: *Treatise on Geochemistry*, edited by Holland, H. D. and Turekian, K. K., Pergamon, Oxford, 2007.

640 Wang, L., Arey, J., and Atkinson, R.: Reactions of chlorine atoms with a series of aromatic hydrocarbons, *Environ. Sci. Technol.*, 39, 5302–5310, <https://doi.org/10.1021/ES0479437>, 2005.

Wang, T., Tham, Y. J., Xue, L., Li, Q., Zha, Q., Wang, Z., Poon, S. C. N., Dubé, W. P., Blake, D. R., Louie, P. K. K., Luk, C. W. Y., Tsui, W., and Brown, S. S.: Observations of nitryl chloride and modeling its source and effect on ozone in the planetary boundary layer of southern China, *Journal of Geophysical Research: Atmospheres*, 121, 2476–2489, <https://doi.org/https://doi.org/10.1002/2015JD024556>, 2016.

645 Wennberg, P. O., Bates, K. H., Crounse, J. D., Dodson, L. G., McVay, R. C., Mertens, L. A., Nguyen, T. B., Praske, E., Schwantes, R. H., Smarte, M. D., St Clair, J. M., Teng, A. P., Zhang, X., and Seinfeld, J. H.: Gas-Phase Reactions of Isoprene and Its Major Oxidation Products, *Chemical Reviews*, 118, 3337–3390, <https://doi.org/10.1021/acs.chemrev.7b00439>, pMID: 29522327, 2018.

Xue, L. K., Saunders, S. M., Wang, T., Gao, R., Wang, X. F., Zhang, Q. Z., and Wang, W. X.: Development of a chlorine chemistry module for the Master Chemical Mechanism, *Geoscientific Model Development*, 8, 3151–3162, <https://doi.org/10.5194/gmd-8-3151-2015>, 2015.

650 Young, C. J., Washenfelder, R. A., Roberts, J. M., Mielke, L. H., Osthoff, H. D., Tsai, C., Pikelnaya, O., Stutz, J., Veres, P. R., Cochran, A. K., VandenBoer, T. C., Flynn, J., Grossberg, N., Haman, C. L., Lefer, B., Stark, H., Graus, M., de Gouw, J., Gilman, J. B., Kuster, W. C., and Brown, S. S.: Vertically Resolved Measurements of Nighttime Radical Reservoirs in Los Angeles and Their Contribution to the Urban Radical Budget, *Environmental Science & Technology*, 46, 10 965–10 973, <https://doi.org/10.1021/es302206a>, pMID: 23013316, 2012.

Zhang, B., Shen, H., Yun, X., Zhong, Q., Henderson, B. H., Wang, X., Shi, L., Gunthe, S. S., Huey, L. G., Tao, S., Russell, A. G., and Liu, P.: 655 Global Emissions of Hydrogen Chloride and Particulate Chloride from Continental Sources, *Environmental Science & Technology*, 56, 3894–3904, <https://doi.org/10.1021/acs.est.1c05634>, pMID: 35319880, 2022.

Zhang, L., Li, Q., Wang, T., Ahmadov, R., Zhang, Q., Li, M., and Lv, M.: Combined impacts of nitrous acid and nitryl chloride on lower-tropospheric ozone: new module development in WRF-Chem and application to China, *Atmospheric Chemistry and Physics*, 17, 9733–9750, <https://doi.org/10.5194/acp-17-9733-2017>, 2017.

660 Zhang, Q., Jimenez, J. L., Canagaratna, M. R., Allan, J. D., Coe, H., Ulbrich, I., Alfarra, M. R., Takami, A., Middlebrook, A. M., Sun, Y. L., Dzepina, K., Dunlea, E., Docherty, K., DeCarlo, P. F., Salcedo, D., Onasch, T., Jayne, J. T., Miyoshi, T., Shimono, A., Hatakeyama, S., Takegawa, N., Kondo, Y., Schneider, J., Drewnick, F., Borrmann, S., Weimer, S., Demerjian, K., Williams, P., Bower, K., Bahreini, R., Cottrell, L., Griffin, R. J., Rautiainen, J., Sun, J. Y., Zhang, Y. M., and Worsnop, D. R.: Ubiquity and dominance of oxygenated species in organic aerosols in anthropogenically-influenced Northern Hemisphere midlatitudes, *Geophysical Research Letters*, 34, L13 801, 665 <https://doi.org/10.1029/2007GL029979>, 2007.